U-Pb zircon geochronology of selected Archaean migmatites in eastern Finland

Asko Käpyaho[1]*, Pentti Hölttä[1], Martin J. Whitehouse[2]

[1] *Geological Survey of Finland, P.O. Box 96, FI-02151 Espoo, Finland*

[2] *Swedish Museum of Natural History, Box 50007, SE-104 05 Stockholm, Sweden*

Abstract

U-Pb SIMS data on eight samples (four mesosome-leucosome pairs) from migmatites in gneiss complexes are presented from the western part of the Archaean Karelian craton, eastern Finland. Most zircon grains in the mesosomes yield ages between 2.84 Ga and 2.79 Ga, with cores of 2.94 Ga in one sample. Age data imply that migmatite mesosome protoliths were generated at broadly the same time as metamorphosed volcanic rocks in the adjacent Kuhmo-Suomussalmi-Tipasjärvi greenstone belt, suggesting that at least some of the mesosomes may represent migmatised equivalents of the greenstone belt rocks. Two separate events of metamorphic zircon growth are recognised from different samples: the first occurred between 2.84 Ga and 2.81 Ga, and the second between 2.73 Ga and 2.70 Ga. The latter event is considered to have led up to a prolonged period of partial melting, as is suggested by the zircons dated from the leucosomes. Scattered age data, inheritance and the large number of discordant data prevented establishing accurate leucosome generation ages. Consequently, the age data are considered to support the previously proposed hypothesis that the Archaean Karelian craton was formed after accumulation of separate tectonic entities having variable ages.

Key words: migmatites, metamorphism, migmatization, absolute age, U/Pb, zircon, Archean, Kuhmo, Lieksa, Finland

*Corresponding author e-mail: asko.kapyaho@gtk.fi

1. Introduction

The western part of the Karelian craton is a typical Archaean gneiss-greenstone terrain consisting of linear greenstone belts surrounded by complexes of TTG (tonalite-trondhjemite-granodiorite) gneisses, migmatites and unmigmatised granitoid rocks (Fig. 1). A variety of formative tectonic environments have been suggested for the greenstone belts. The Kuhmo-Suomussalmi-Tipasjärvi belt (referred to here as the Kuhmo greenstone belt; Fig. 2) has been variably attributed to intracontinental rifting (Martin et al., 1984; Luukkonen 1992, 2001), aborted rifting preceded and followed by subduction (Piirainen, 1988), island arc magmatism (Taipale 1983, 1988), and back-arc rifting (Gaál & Gorbatschev, 1987). In addition, Kontinen et al. (2007) have suggested that the Nurmes paragneisses (Fig. 2), which are most prominent to the southeast of the Kuhmo greenstone belt, were deposited in a back-arc or intra-arc tectonic setting.
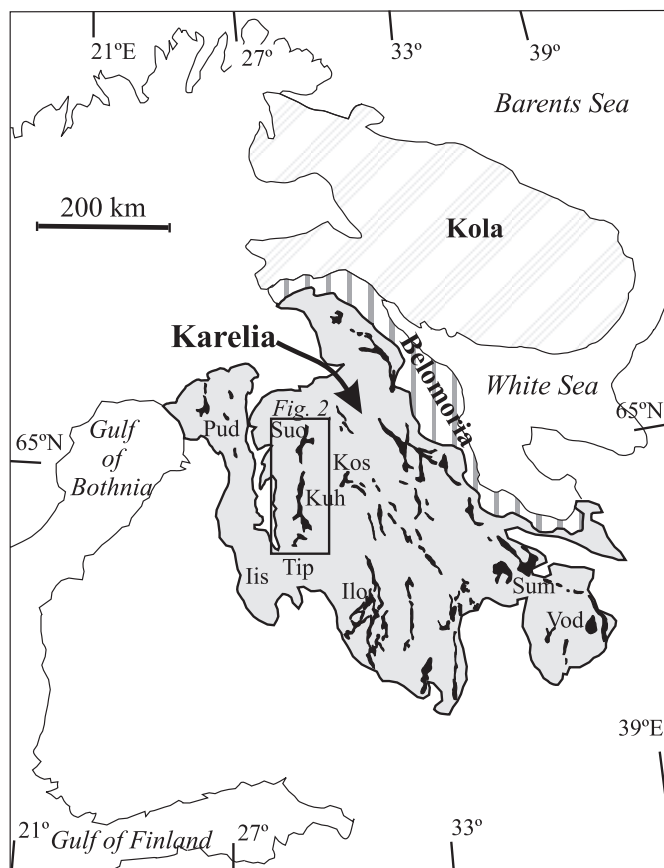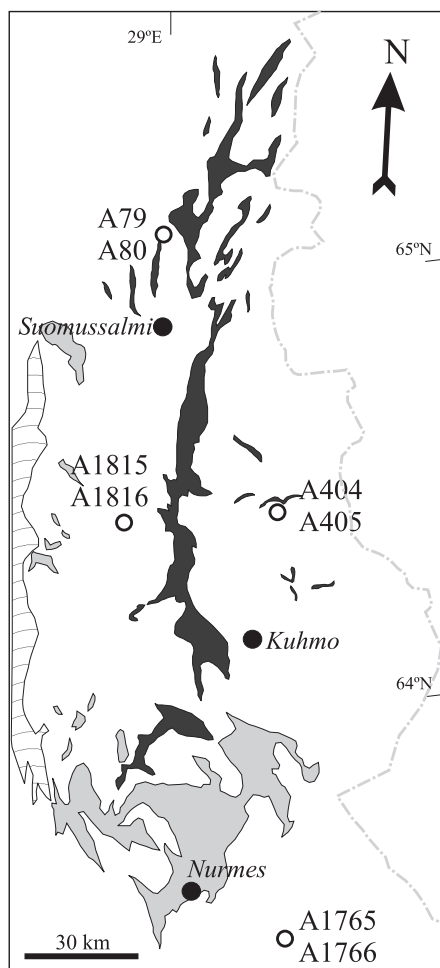
Fig. 1. Generalised bedrock map showing the main Archaean crustal domains of the Fennoscandian Shield (modified after Koistinen et al., 2001) and the main Archaean greenstone belts. Abbreviations are Pud = Pudasjärvi block, Iis = Iisalmi block, Tip = Tipasjärvi greenstone belt, Kuh = Kuhmo greenstone belt, Suo = Suomussalmi greenstone belt, Kos = Kostomuksha greenstone belt, Ilo = Ilomantsi greenstone belt, Sum = Sumozero greenstone belt, and Vod = Vodlozero block.

In general, the age relationships between the greenstone belts and the surrounding bedrock are crucial for understanding of the tectonic setting(s) of the granite-greenstone terranes. In the Kuhmo district, the migmatitic TTG gneisses or associated banded amphibolites have been considered as the oldest rocks in the area (cf. Martin et al., 1984; Luukkonen, 1992). Previously reported age determinations from the migmatites are based on conventional multigrain U-Pb analyses (Luukkonen, 1985) and whole-rock Rb-Sr method (e.g. Martin, 1985). Of these two methods, the Rb-Sr method has often been shown to give younger ages compared to the U-Pb method (Vaasjoki, 1988; Halliday et al., 1988); however, the age relationships determined by both these methods for plutonic phases are fairly similar. Furthermore, multiple zircon growth episodes, which are often reported in Archaean polydeformed terrains (e.g. Whitehouse & Kamber, 2005), complicate the interpretation of results obtained from the conventional TIMS (thermal ionisation mass spectrometer) U-Pb method. In order to overcome these technical restrictions, we have performed U-Pb SIMS (secondary ion mass spectrometer) dating on zircons from leucosome-mesosome pairs of migmatites surrounding the Kuhmo greenstone belt.

Fig. 2. Generalised bedrock map from Kuhmo district (modified after Korsman et al., 1997) showing sampling locations.

This study has two main goals. First, by dating zircons from mesosomes, our purpose is to compare their protolith ages with the ages of granitoid and volcanic rocks of the Kuhmo district, and thereby evalu-

ate the relationship between the greenstone belt and the surrounding bedrock. Second, by dating zircons from leucosomes, we aim to date the high-grade metamorphism and related melting events, and study their timing with respect to known main magmatic events within the study area.

2. Geological setting and geochronological background

The Archaean bedrock in the Fennoscandian Shield is commonly divided into three main crustal units: the Kola, Belomorian and Karelian provinces (e.g. Gaál & Gorbatschev, 1987). The Karelian province (craton) consists of Palaeoarchaean to Neoarchaean greenstone belts, migmatites, TTG gneisses and migmatites, amphibolites and granitoid rocks (e.g. Gaál & Gorbatschev, 1987; Martin, 1987). The province is bordered by Palaeoproterozoic Svecofennian rocks in the west and Neoarchaean rocks belonging to Belomorian mobile belt in the east (e.g. Evins et al., 2002). The largest presently known occurrences of Mesoarchaean to Palaeoarchaean rocks are the gneisses exposed in the Vodlozero block in the southeastern part of the Karelian province (Lobach-Zhuchenko et al., 1993; Sergeev et al., 1990) and its westernmost part within the Iisalmi (Hölttä et al., 2000) and Pudasjärvi blocks (Mutanen & Huhma, 2003). In the Iisalmi block, the 3.2 – 3.1 Ga amphibolite-banded gneisses are considered to have been juxtaposed with the 2.7 – 2.8 Ga ortho- and paragneisses as a result of terrane accretion that preceded the granulite facies metamorphic event at 2.70 – 2.63 Ga (Hölttä et al., 2000; Hölttä & Paavola, 2000; Mänttäri & Hölttä, 2002). Migmatite protoliths with such old ages are not known from the Kuhmo district; the conventional U-Pb zircon age of 2.84 Ga for a mesosome of a migmatite located in Lylyvaara (A404 in Fig. 2) represents the oldest mesosome age obtained so far.

The numerous linear and discontinuous greenstone belts in the Karelian craton are generally N-trending, and their ages vary from Mesoarchaean to Neoarchaean (Puchtel et al., 1997; Sorjonen-Ward et al., 1997; Sorjonen-Ward & Luukkonen, 2005). For

example, the felsic volcanic rocks in the Suomussalmi greenstone belt (Fig. 1) have yielded reliable U-Pb zircon and monazite ages of ca. 3.0 – 2.82 Ga (Huhma et al., 1999; Luukkonen et al., 2002). Conventional U-Pb zircon ages for the felsic and mafic volcanic rocks in the Kuhmo and Tipasjärvi greenstone belts are between ca. 3.01 – 2.79 Ga (Hyppönen, 1983; Luukkonen, 1988; Vaasjoki et al., 1999; Luukkonen et al., 2002). Vaasjoki et al. (1993) reported a U-Pb age of 2.75 Ga for a meta-andesite sample from the Ilomantsi greenstone belt, which is thus far the youngest volcanic age reported from the Archaean greenstone belts of eastern Finland. A minimum age for the mafic volcanic rocks of the Kuhmo greenstone belt is constrained by a crosscutting quartz diorite dyke dated at 2.74 Ga by using the U-Pb method on zircon and titanite (Hyppönen, 1983).

Unmigmatised granitoid plutons within and surrounding the greenstone belts in the western part of the Karelian craton, as in the Kuhmo and Ilomantsi areas, have ages between 2.83 Ga and 2.68 Ga. These plutonic rocks appear to show a compositional trend through time from tonalites and trondhjemites varying in age between 2.83 Ga and 2.75 Ga (Hyppönen, 1983; Luukkonen, 1988; Vaasjoki et al., 1993, 1999; Samsonov et al., 2005; Käpyaho et al., 2006) to high-Mg/Fe granitoid rocks (sanukitoid suites) at 2.74 – 2.70 Ga (Bibikova et al., 2005, Halla 2002, 2005; Käpyaho, 2006). The youngest Neoarchaean granitoid rocks are leucocratic granites and granodiorites dated between 2.70 Ga and 2.68 Ga (e.g., Käpyaho et al., 2006; Lauri et al., 2006).

During Palaeoproterozoic time, the Karelian craton was intruded by 2.44 Ga mafic layered intrusions and A-type granites as well as several swarms of 2.44 – 1.96 Ga metadiabase dikes (Vuollo & Huhma, 2005; Lauri & Mänttäri, 2002; Luukkonen, 1988; Vuollo, 1994; Alapieti, 1982). These magmatic episodes are considered to evidence repeated Palaeoproterozoic rifting of the Archaean craton (e.g. Vuollo & Huhma, 2005). The western part of the province was variably reworked during the Svecofennian orogeny under greenschist to low amphibolite facies thermal conditions at about 1.9 Ga, causing resetting of

K-Ar systematics in Neoarchaean rocks (Kontinen et al., 1992).

3. Sample description

Four migmatite mesosome-leucosome pairs were selected for U-Pb SIMS dating from eastern Finland (Fig. 2; Table 1). The Myllykynnäs samples (A1815 and A1816) and Päivärinta samples (A79 and A80) are from the western side of the Kuhmo greenstone belt, whereas the Lylyvaara samples (A404 and A405) come from eastern side of the belt. The Jamali samples (A1765 and A1766) are from Lieksa, southeast of the Kuhmo greenstone belt. The Lylyvaara and Päivärinta samples were collected and dated by TIMS multigrain method before the initiation of this study. The U-Pb data for the Lylyvaara migmatite are presented by Luukkonen (1985) and results for the Päivärinta migmatite are briefly summarised by Luukkonen et al. (2002) and presented here in Table 2. All these conventional data are also shown in the concordia plots below. Sample locations are shown in Figure 2.

3.1. A1815 and A1816, Myllykynnäs

The Myllykynnäs migmatite is a stromatic metatexite in which the thickness of individual mesosome and leucosome layers varies between < 1 cm and 20 cm (Fig. 3a). Mesosome A1815 is medium grained and the main minerals are plagioclase, biotite and quartz. Leucosome A1816 is a pinkish granite comprising fine grained microcline and quartz as the main minerals.

3.2. A1765 and A1766, Jamali

The Jamali migmatite is also a stromatic metatexite (Fig. 3b). The mesosomes show locally faint layering defined by alternating darker and lighter layers. Mesosome A1765 is medium grained; the main minerals are plagioclase, quartz and biotite. Retrograde epidote is common. Leucosome A1766 is medium to coarse grained and the main minerals are plagioclase
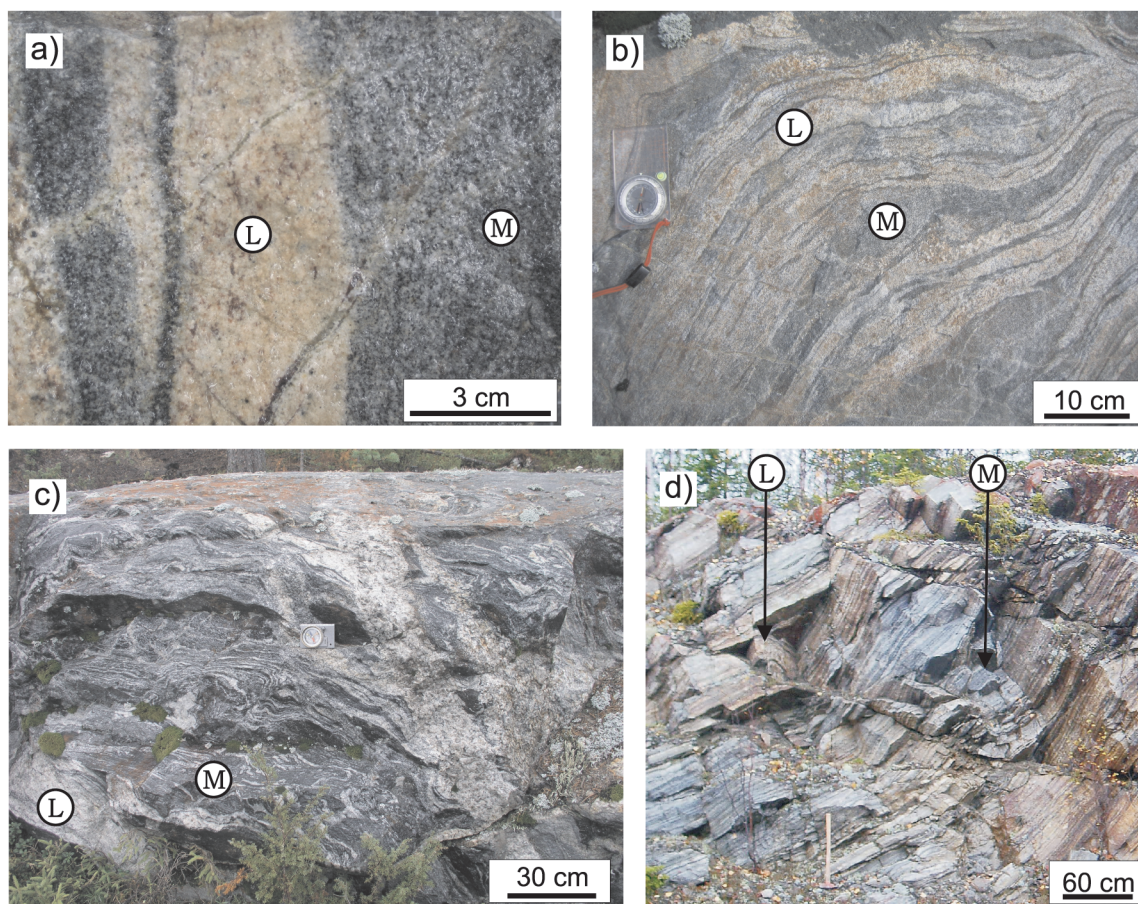
Fig. 3. Photographs showing the dated sample (a) or the exposures, where the samples have been taken (b-d). L and M denote typical leucosomes and mesosomes, respectively, but not necessarily the exact sampling locations. a) Myllykynnäs (A1815 and 1816), b) Jamali (A1765 and A1766), c) Lylyvaara (A404 and 405) and d) Päivärinta (A79 and A80).

and quartz. Biotite, retrograde epidote and retrograde muscovite are accessory minerals.

3.3. A404 and A405, Lylyvaara

The Lylyvaara migmatite is a polydeformed diatexitic migmatite (Fig. 3c). Mesosome sample A404 is grey-ish or dark, medium grained and granoblastic and consists of biotite, hornblende, quartz and plagiocla-se. Leucosome sample A405 is a leucocratic granite, comprising medium to coarse grained quartz and mi-crocline. More detailed sample descriptions and con-ventional multigrain data for both mesosome A404 and leucosome A405 are presented by Luukkonen

(1985). The same zircon separates as studied by Luuk-konen (*op.cit.*) were used in this study; density frac-tion $4.1 < \rho < 4.6$ from mesosome A404 and densi-ty fractions $\rho < 4.1$ and $4.1 < \rho < 4.2$ from leuco-some A405.

3.4. A79 and A80, Päivärinta

The Päivärinta migmatite is a granoblastic, fine to medium grained stromatic metatexite (Fig. 3d). The thickness of individual mesosome and leuco-some layers varies between < 1 cm and 10 cm. The main minerals in the mesosome A79 are plagioclase, quartz, and biotite. Leucosome A80 is a granoblastic,

Table I. SIMS U-Th-Pb data for zircons.

Sample/ spot #	Spot site* Description	derived ages $^{207}Pb/^{206}Pb$	±σ	corrected ratios $^{207}Pb/^{206}Pb$ ±σ %	$^{207}Pb/^{235}U$ ±σ %	$^{206}Pb/^{238}U$ ±σ %	ρ	Disc. % 2σ lim.	elemental data [U] ppm	[Th] ppm	[Pb] ppm	$^{206}Pb/^{204}Pb$ meas.	Th/U meas.
A1815 mesosome													
n1529-11a	oz p	2819	6	0.1991 0.38	15.13 1.8	0.5513 1.8	0.98		167	119	128	15860	0.71
n1529-12a	oz p	2817	6	0.1989 0.38	15.23 1.8	0.5556 1.8	0.98		175	132	137	30925	0.75
n1529-15a	oz p	2814	7	0.1985 0.45	14.90 1.6	0.5443 1.6	0.96		134	82	99	89180	0.61
n1529-05a	oz p	2813	6	0.1983 0.38	15.14 1.8	0.5535 1.8	0.98		153	88	114	28366	0.58
n1529-06a	lz p	2810	7	0.1980 0.43	15.72 1.9	0.5760 1.8	0.97	1.3	155	93	121	2593	0.60
n1529-14a	oz p	2806	9	0.1975 0.56	13.81 1.6	0.5072 1.5	0.94	-3.4	138	59	93	2408	0.42
n1646-24a	oz p	2803	7	0.1972 0.41	14.51 1.2	0.5338 1.1	0.94		83	46	60	3602	0.55
n1646-26a	oz p	2802	5	0.1971 0.30	14.86 1.2	0.5469 1.2	0.97		116	54	84	28985	0.47
n1529-16a	oz p	2802	7	0.1970 0.44	15.16 1.6	0.5581 1.5	0.96		170	122	131	41932	0.72
n1529-10a	oz p	2801	6	0.1969 0.38	14.92 1.8	0.5493 1.8	0.98		163	127	125	31678	0.78
n1529-08a	oz p	2801	7	0.1969 0.42	14.80 1.9	0.5452 1.8	0.97		140	107	107	17351	0.76
n1646-22a	oz p	2801	5	0.1969 0.31	14.85 1.2	0.5469 1.2	0.97		150	94	113	14139	0.62
n1529-18a	oz p	2800	7	0.1969 0.44	15.00 1.6	0.5528 1.6	0.96		170	92	125	15710	0.54
n1529-13a	oz p	2799	7	0.1967 0.41	14.72 1.2	0.5428 1.1	0.94		178	137	135	1937	0.77
n1646-27a	oz p	2799	5	0.1967 0.33	13.87 1.2	0.5116 1.1	0.96	-3.4	136	81	95	3682	0.60
n1529-07a	oz p	2797	11	0.1965 0.70	14.80 1.9	0.5462 1.8	0.93		59	34	44	13261	0.57
n1646-25a	oz p	2796	7	0.1964 0.43	14.86 1.2	0.5488 1.1	0.94		104	41	74	6752	0.39
n1529-19a	oz p	2795	7	0.1962 0.45	14.84 1.6	0.5486 1.5	0.96		158	85	116	15964	0.54
n1529-01a	oz	2795	11	0.1962 0.68	14.13 1.9	0.5222 1.8	0.94		81	39	56	14224	0.48
n1646-20a	oz	2790	6	0.1956 0.36	15.68 1.2	0.5816 1.1	0.95	4.6	167	91	131	2488	0.54
n1646-23a	oz p	2777	5	0.1941 0.31	13.94 1.2	0.5209 1.2	0.97	-0.7	196	90	135	3292	0.46
n1529-17a	oz p	2775	10	0.1938 0.59	14.73 1.7	0.5511 1.6	0.94		86	41	63	14402	0.48
n1529-09a	oz p	2742	13	0.1899 0.78	13.59 2.0	0.5190 1.9	0.92		48	17	32	4775	0.35
n1646-28a	m	2740	4	0.1898 0.26	13.71 1.2	0.5240 1.2	0.98		248	183	182	2707	0.74
Data ignored due to high discordance or low $^{206}Pb/^{204}Pb$													
n1529-02a	*nz c*	*2666*	*39*	*0.1814 2.4*	*7.437 3.0*	*0.2973 1.8*	*0.61*	*-32.4*	*32*	*7*	*12*	*386*	*0.21*
n1646-21a	*oz p*	*2742*	*60*	*0.1900 3.7*	*11.89 4.0*	*0.4540 1.5*	*0.38*	*disk*	*154*	*88*	*95*	*199*	*0.57*
n1646-29a	*oz*	*2815*	*6*	*0.1987 0.34*	*15.07 1.2*	*0.5499 1.1*	*0.96*		*147*	*85*	*109*	*820*	*0.58*
n1529-04a	*oz p*	*2706*	*10*	*0.1859 0.58*	*10.64 1.9*	*0.4152 1.8*	*0.95*	*-16.7*	*151*	*77*	*84*	*3344*	*0.51*
n1529-03a	*oz p*	*2815*	*7*	*0.1986 0.43*	*12.14 1.9*	*0.4432 1.8*	*0.97*	*-15.7*	*275*	*225*	*173*	*20258*	*0.82*
A1816 leucosome													
n1530-01a	w oz c p	2698	3	0.1850 0.17	13.53 1.1	0.5302 1.1	0.99		1609	86	1023	73160	0.053
n1530-02a	mm a	2682	2	0.1832 0.13	13.00 1.1	0.5148 1.1	0.99		1315	85	811	11365	0.064
n1530-06a	mm a	2674	3	0.1823 0.19	12.42 1.6	0.4939 1.5	0.99	-0.9	1475	51	867	5356	0.035
n1530-05a	mm a	2618	3	0.1763 0.19	10.95 1.6	0.4508 1.5	0.99	-7.1	1957	54	1044	4742	0.027
n1530-04a	mm a	2610	11	0.1754 0.67	10.65 1.7	0.4401 1.5	0.92	-8.0	2236	71	1161	1107	0.032
n1645-20a	mm p	2531	18	0.1673 1.1	9.439 2.4	0.4092 2.1	0.89	-9.3	2144	68	1031	5790	0.032
n1645-23a	mm a	2423	11	0.1570 0.63	8.964 1.7	0.4142 1.5	0.93	-5.4	3821	1193	2070	12274	0.31
Data ignored due to high discordance or low $^{206}Pb/^{204}Pb$													
n1645-24a	*mm p*	*2515*	*16*	*0.1657 0.94*	*4.992 1.8*	*0.2185 1.5*	*0.85*	*-50.0*	*2170*	*261*	*561*	*540*	*0.12*
n1645-25a	*mm p*	*2541*	*61*	*0.1683 3.7*	*5.851 3.9*	*0.2522 1.2*	*0.30*	*-32.9*	*1559*	*47*	*480*	*87*	*0.030*
n1645-26a	*mm a*	*2604*	*12*	*0.1748 0.70*	*5.033 1.5*	*0.2089 1.4*	*0.89*	*-54.9*	*967*	*33*	*240*	*244*	*0.034*
n1645-22a	*mm a*	*2419*	*6*	*0.1566 0.37*	*5.764 1.7*	*0.2669 1.6*	*0.98*	*-38.9*	*2937*	*143*	*916*	*666*	*0.049*
n1530-01b	*w oz og p*	*2538*	*3*	*0.1680 0.20*	*7.851 1.1*	*0.3389 1.1*	*0.98*	*-28.0*	*3077*	*204*	*1236*	*6543*	*0.066*
n1530-07a	*mm p*	*2602*	*4*	*0.1745 0.24*	*7.381 1.6*	*0.3067 1.5*	*0.99*	*-36.2*	*1651*	*205*	*605*	*1489*	*0.12*
n1530-03a	*w oz p*	*2655*	*6*	*0.1802 0.34*	*11.50 1.6*	*0.4630 1.5*	*0.98*	*-6.0*	*903*	*30*	*494*	*391*	*0.034*
n1530-08a	*w oz p*	*2785*	*13*	*0.1950 0.79*	*11.57 1.7*	*0.4301 1.5*	*0.89*	*-16.5*	*154*	*110*	*91*	*528*	*0.72*
n1530-09a	*nz a*	*2586*	*24*	*0.1729 1.4*	*10.68 2.1*	*0.4483 1.6*	*0.74*	*-2.7*	*88*	*25*	*49*	*400*	*0.29*
n1530-10a	*wz a*	*2798*	*33*	*0.1966 2.1*	*15.39 2.6*	*0.5679 1.6*	*0.60*		*86*	*59*	*67*	*246*	*0.68*
n1645-21a	*w oz*	*2563*	*2*	*0.1706 0.14*	*9.263 1.2*	*0.3938 1.1*	*0.99*	*-17.4*	*1245*	*86*	*582*	*6050*	*0.069*
A1765 mesosome													
n1531-06a	nz c i	2845	5	0.2023 0.29	15.69 1.6	0.5624 1.5	0.98		364	215	279	19400	0.59
n1531-10a	wz p	2828	4	0.2002 0.27	15.61 1.6	0.5654 1.6	0.98		511	216	381	92887	0.42
n1531-03a	nz c p	2814	4	0.1985 0.25	13.53 1.6	0.4944 1.5	0.99	-6.7	800	230	504	7229	0.29
n1531-11a	oz p	2803	13	0.1972 0.79	14.52 1.7	0.5339 1.5	0.89		49	24	35	13604	0.50
n1647-21a	w oz p	2802	6	0.1970 0.34	14.76 1.3	0.5431 1.2	0.96		105	41	74	13814	0.39
n1531-02a	oz p	2799	8	0.1967 0.51	14.90 1.6	0.5495 1.6	0.95		112	88	87	48010	0.78
n1531-04a	oz p	2793	12	0.1960 0.75	14.80 1.7	0.5477 1.6	0.90		69	43	51	16491	0.63
n1531-09a	oz p	2791	12	0.1957 0.75	14.80 1.7	0.5484 1.5	0.90		111	83	85	13071	0.75
n1531-08a	oz a	2788	12	0.1954 0.74	14.79 1.7	0.5490 1.5	0.90		57	28	41	6799	0.49
n1647-20a	mm a	2785	3	0.1950 0.19	13.25 1.2	0.4928 1.1	0.99	-6.6	354	121	226	6450	0.34
n1531-01a	oz p	2784	8	0.1949 0.48	15.20 1.6	0.5654 1.5	0.95	0.9	120	81	93	22374	0.67
n1647-26a	oz p	2784	6	0.1949 0.36	14.62 1.2	0.5441 1.2	0.95		101	70	76	4746	0.69
n1531-07a	oz p	2781	10	0.1946 0.59	14.70 1.7	0.5477 1.5	0.93		90	48	66	20044	0.53
n1647-24a	oz p	2781	8	0.1946 0.51	14.70 1.3	0.5478 1.2	0.91		82	60	63	4482	0.73
n1647-25a	wz c p	2769	3	0.1932 0.17	12.91 1.2	0.4846 1.1	0.99	-7.5	682	256	425	31930	0.38
n1531-12a	oz c	2767	13	0.1929 0.82	14.34 1.8	0.5394 1.6	0.89		61	34	44	10111	0.56
n1647-22a	oz p	2767	4	0.1929 0.27	13.75 1.2	0.5170 1.1	0.97	-1.1	236	59	152	1468	0.25
n1531-05a	oz a	2761	11	0.1922 0.64	15.07 1.7	0.5684 1.5	0.92	2.1	98	57	74	2954	0.58
n1647-23a	nz c p	2711	6	0.1865 0.18	12.25 1.5	0.4763 1.5	0.99	-6.1	953	413	583	2071	0.43
Data ignored due to high discordance or low $^{206}Pb/^{204}Pb$													
n1647-27a	*oz p*	*2766*	*6*	*0.1928 0.40*	*11.53 1.3*	*0.4339 1.2*	*0.95*	*-16.5*	*84*	*44*	*48*	*3165*	*0.52*
A1766 leucosome													
n1648-25a	w oz p	2839	2	0.2016 0.12	15.05 1.2	0.5414 1.1	0.99		863	927	696	49763	1.1
n1532-06a	mm a i	2826	3	0.2000 0.21	14.09 1.6	0.5109 1.5	0.99	-4.2	855	469	585	19628	0.55
n1532-05a	w oz p	2806	2	0.1976 0.14	15.40 1.6	0.5654 1.5	1.00	0.4	1769	2030	1501	67426	1.1
n1648-21a	w oz p	2803	1	0.1971 0.07	15.37 1.1	0.5655 1.1	1.00	1.5	1601	843	1209	385625	0.53
n1648-26a	w oz p	2797	1	0.1965 0.09	14.55 1.2	0.5369 1.2	1.00		1330	137	876	92091	0.10
n1648-23a	w oz p	2795	1	0.1962 0.12	14.96 1.1	0.5529 1.1	0.99		1255	313	888	17487	0.25
n1532-10a	oz a	2791	5	0.1958 0.29	13.85 1.6	0.5132 1.5	0.98	-2.2	579	184	379	5482	0.32
n1532-02a	oz p	2787	7	0.1952 0.42	14.84 1.6	0.5514 1.5	0.97		192	133	145	2383	0.69
n1532-04a	oz p	2779	9	0.1943 0.54	13.85 1.7	0.5170 1.6	0.95	-0.4	115	58	79	3727	0.50
n1532-08a	w oz p	2776	4	0.1939 0.27	14.55 1.6	0.5443 1.6	0.98		552	20	360	5312	0.036
n1648-24a	oz p	2770	5	0.1932 0.29	13.62 1.2	0.5112 1.1	0.97	-2.3	141	94	99	11876	0.67
n1648-22a	nz a	2714	1	0.1868 0.07	13.58 1.2	0.5273 1.2	1.00		2447	100	1547	12763	0.04
n1532-17a	mm p	2707	2	0.1860 0.14	14.06 1.6	0.5482 1.5	1.00	1.7	2478	120	1627	48272	0.048
n1532-16a	mm p	2707	2	0.1860 0.11	13.98 1.5	0.5451 1.5	1.00	1.2	2911	184	1907	81627	0.063
n1532-11a	mm p	2706	2	0.1859 0.12	12.67 1.6	0.4944 1.5	1.00	-2.3	2499	91	1477	84359	0.036
n1532-14a	mm p	2691	2	0.1842 0.11	13.86 1.5	0.5456 1.5	1.00	2.0	2816	149	1840	222679	0.053
n1532-15a	nz p	2683	2	0.1833 0.15	13.42 1.6	0.5309 1.6	1.00		1537	95	980	64094	0.062
n1532-18a	mm p	2633	2	0.1778 0.13	11.23 1.6	0.4579 1.5	1.00	-6.4	3811	280	2089	44389	0.074
n1532-03a	mm a	2226	4	0.1399 0.21	8.510 1.6	0.4412 1.5	0.99	3.5	13305	954	6802	102013	0.072

Table 1. cont. SIMS U-Th-Pb data for zircons.

Sample/ spot #	Spot site* Description	derived ages				corrected ratios					Disc. % 2σ lim.	elemental data				Th/U
		^{207}Pb / ^{206}Pb	±σ	^{207}Pb / ^{206}Pb	±σ %	^{207}Pb / ^{235}U	±σ %	^{206}Pb / ^{238}U	±σ %	ρ		[U] ppm	[Th] ppm	[Pb] ppm	$^{206}Pb/^{204}Pb$ meas.	meas.
Data ignored due to high discordance or low $^{206}Pb/^{204}Pb$																
n1648-20a	oz p	2748	90	0.1906	5.7	13.58	5.8	0.5168	1.2	0.20		113	49	74	149	0.43
n1648-27a	nz a	2483	15	0.1626	0.92	8.212	3.9	0.3663	3.7	0.97	-15.1	2112	264	928	835	0.12
n1532-09a	w oz p	2730	3	0.1886	0.17	10.46	1.6	0.4024	1.6	0.99	-21.2	1911	84	919	3966	0.044
n1532-07a	oz p	2768	6	0.1930	0.38	12.06	1.6	0.4531	1.6	0.97	-12.5	532	430	331	1234	0.81
n1532-12a	mm p	2678	5	0.1828	0.30	10.48	1.6	0.4160	1.5	0.98	-16.5	2342	143	1172	1394	0.061
n1532-01a	wz c i	2406	5	0.1554	0.27	8.092	1.6	0.3777	1.6	0.99	-13.6	3138	939	1453	84963	0.30
A404 mesosome																
n1533-08a	oz c p	2949	8	0.2157	0.49	17.58	1.7	0.5913	1.6	0.96		137	97	114	38682	0.71
n1533-02a	w oz c p	2944	3	0.2150	0.18	17.71	1.6	0.5974	1.6	0.99		883	589	737	78121	0.67
n1533-07a	w oz c p	2941	6	0.2146	0.35	17.32	1.6	0.5854	1.6	0.98		287	145	227	30215	0.51
n1533-01a	oz c p	2939	5	0.2144	0.31	17.78	1.6	0.6016	1.6	0.98	0.7	443	318	376	34326	0.72
n1533-05a	w oz c p	2937	8	0.2141	0.47	16.54	1.7	0.5601	1.6	0.96		192	145	151	5567	0.75
n1533-04a	oz c p	2935	8	0.2139	0.52	17.50	1.7	0.5934	1.6	0.95		134	115	115	19723	0.86
n1533-09a	oz c p	2931	8	0.2133	0.48	17.18	1.6	0.5840	1.6	0.96		142	103	117	10220	0.73
n1533-10a	w oz c?	2898	5	0.2091	0.30	16.52	1.6	0.5729	1.6	0.98		389	350	324	19775	0.90
n1533-06a	w oz c p	2867	8	0.2051	0.46	15.34	1.6	0.5426	1.6	0.96		357	165	259	7606	0.46
n1533-01b	h og p	2839	3	0.2016	0.21	15.94	1.6	0.5734	1.6	0.99	0.3	737	8	508	40201	0.010
n1533-03a	w oz c p	2833	4	0.2008	0.27	15.66	1.6	0.5656	1.6	0.99		452	301	357	19403	0.67
n1533-08b	h og p	2817	6	0.1989	0.38	15.36	1.6	0.5603	1.6	0.97		521	8	351	23232	0.016
n1533-03b	wz og p	2809	6	0.1979	0.36	15.20	1.6	0.5571	1.6	0.98		297	3	198	27851	0.010
n1533-07b	wz og p	2806	8	0.1976	0.47	14.91	1.7	0.5472	1.6	0.96		177	1	[116]	20959	0.006
A405 leucosome																
n1534-09a	mm p	2739	3	0.1897	0.17	14.50	1.6	0.5546	1.6	0.99	1.4	1333	109	895	73856	0.08
n1534-08a	nz p	2697	3	0.1848	0.19	13.85	1.6	0.5434	1.6	0.99	1.2	2152	404	1444	112698	0.19
n1534-10a	w oz p	2646	4	0.1793	0.21	11.85	1.6	0.4793	1.6	0.99	-2.5	1783	139	1024	50958	0.08
n1534-12a	wz p	2620	3	0.1765	0.21	12.77	1.6	0.5247	1.6	0.99	1.2	2430	419	1558	109006	0.17
n1534-07a	nz p	2576	3	0.1719	0.17	11.99	1.6	0.5060	1.6	0.99		2796	564	1734	137731	0.20
n1534-06a	nz p	2567	3	0.1709	0.16	11.92	1.6	0.5060	1.6	1.00	0.1	3339	445	2037	102962	0.13
n1534-02a	nz p	2544	2	0.1686	0.15	10.55	1.6	0.4537	1.6	1.00	-3.2	2555	448	1409	15009	0.18
n1534-04a	nz p	2517	4	0.1660	0.21	10.86	1.6	0.4744	1.6	0.99		1806	225	1026	4848	0.12
n1534-05a	w oz p	2489	3	0.1632	0.16	10.96	1.6	0.4870	1.6	1.00	0.0	3535	518	2071	75367	0.15
n1534-03a	w oz p	2450	3	0.1595	0.15	10.81	1.6	0.4916	1.6	1.00	2.9	4979	870	2955	72359	0.17
n1534-13a	mm p	2421	3	0.1568	0.20	10.34	1.6	0.4784	1.6	0.99	1.5	5472	947	3150	86469	0.17
n1534-11a	mm a	2410	4	0.1557	0.24	10.43	1.6	0.4859	1.6	0.99	3.7	4752	1002	2780	2238	0.21
n1534-01a	mm p	2232	3	0.1404	0.19	7.431	1.6	0.3839	1.6	0.99	-4.2	6460	1296	2941	732	0.20
A79 mesosome																
n1535-03a	oz p	2846	10	0.2024	0.64	15.66	1.7	0.5612	1.6	0.93		98	45	73	7463	0.46
n1535-07a	nz p	2842	3	0.2019	0.21	15.37	1.6	0.5521	1.6	0.99		1167	930	910	56571	0.80
n1644-22a	w oz a	2841	3	0.2019	0.16	15.46	1.9	0.5553	1.9	1.00		1168	849	908	16337	0.73
n1644-27b	wz a	2841	4	0.2018	0.24	15.40	1.9	0.5535	1.9	0.99		291	107	210	17034	0.37
n1644-23a	oz p	2841	3	0.2018	0.21	15.68	1.9	0.5636	1.9	0.99		311	154	233	9857	0.50
n1535-02a	oz p	2839	3	0.2016	0.17	15.95	1.6	0.5738	1.6	0.99	0.3	1222	637	939	66409	0.52
n1644-24a	oz p	2838	4	0.2014	0.23	15.44	1.9	0.5558	1.9	0.99		487	320	371	4193	0.66
n1535-01a	wz c	2838	4	0.2014	0.26	15.81	1.6	0.5692	1.6	0.99		655	274	489	18732	0.42
n1644-20b	wz a	2837	3	0.2014	0.19	15.77	1.9	0.5678	1.9	0.99		632	240	468	53702	0.38
n1644-34a	nz p	2837	3	0.2013	0.16	14.82	1.9	0.5340	1.9	1.00		1234	340	837	76449	0.28
n1535-06a	oz p	2836	5	0.2012	0.32	15.83	1.6	0.5704	1.6	0.98		495	325	388	49947	0.66
n1644-26a	oz p	2835	4	0.2010	0.27	15.31	1.9	0.5522	1.9	0.99		290	84	204	29971	0.29
n1644-25a	w oz a	2834	4	0.2009	0.22	15.36	1.9	0.5544	1.9	0.99		324	222	248	9011	0.69
n1535-05a	w oz a	2832	9	0.2007	0.56	15.04	1.7	0.5433	1.6	0.94		210	119	154	2190	0.57
n1644-32a	nz c? p	2831	2	0.2006	0.14	15.30	1.9	0.5532	1.9	1.00		753	333	550	15692	0.44
n1644-21a	oz a	2828	3	0.2002	0.18	15.73	1.9	0.5696	1.9	1.00		411	232	317	23392	0.56
n1535-08a	w oz p	2816	4	0.1988	0.22	13.16	1.6	0.4800	1.6	0.99	-9.5	930	348	580	23344	0.37
n1644-33a	oz c	2813	8	0.1984	0.48	14.83	1.9	0.5424	1.9	0.97		97	33	68	5599	0.34
n1644-20a	wz a	2799	3	0.1967	0.18	15.14	1.9	0.5580	1.9	1.00		639	20	[431]	2310	0.032
n1644-28a	oz c p	2796	4	0.1964	0.25	14.76	1.9	0.5452	1.9	0.99		375	216	278	16425	0.58
n1535-04a	oz p	2795	10	0.1963	0.60	14.90	1.7	0.5504	1.6	0.94		108	76	82	8129	0.70
n1535-01b	nz og	2726	4	0.1881	0.23	13.99	1.6	0.5395	1.6	0.99		815	0	[522]	66565	<0.001
n1644-29a	nz og	2718	2	0.1873	0.13	13.84	1.9	0.5358	1.9	1.00		2489	628	1673	181974	0.25
n1644-27a	wz a og	2714	2	0.1867	0.11	13.79	1.9	0.5356	1.9	1.00		1112	4	707	62385	0.0039
n1644-31a	nz og p	2698	2	0.1850	0.13	12.75	1.9	0.4999	1.9	1.00	-0.2	1391	271	862	19071	0.19
Data ignored due to high discordance or low $^{206}Pb/^{204}Pb$																
n1644-21b	oz a	2812	12	0.1983	0.76	13.01	2.0	0.4759	1.9	0.93	-8.6	184	60	113	442	0.32
A80 leucosome																
n1643-05a	w oz p	2846	2	0.2024	0.12	15.43	1.9	0.5529	1.9	1.00		1602	1448	1282	58904	0.90
n1643-04a	w oz p	2827	5	0.2002	0.31	14.82	1.9	0.5370	1.9	0.99		184	167	143	11084	0.91
n1643-03a	w oz? p	2779	2	0.1943	0.14	14.24	1.9	0.5315	1.9	1.00		904	79	584	19431	0.088
n1643-15a	nz p	2772	2	0.1935	0.14	14.45	1.9	0.5418	1.9	1.00		867	45	567	9226	0.052
n1643-06a	nz a	2772	5	0.1934	0.33	13.54	1.9	0.5077	1.9	0.98	-1.7	648	39	397	1248	0.060
n1643-07a	nz a	2761	3	0.1922	0.18	13.44	1.9	0.5070	1.9	1.00	-1.6	812	99	503	2179	0.12
n1643-16a	nz a	2740	2	0.1897	0.12	14.21	1.9	0.5433	1.9	1.00		1287	102	845	7132	0.079
n1643-12a	w oz p	2713	5	0.1867	0.29	12.16	1.9	0.4722	1.9	0.99	-6.2	568	209	345	7649	0.37
n1643-20a	wz p	2698	5	0.1850	0.21	13.49	1.9	0.5291	1.9	0.99		340	532	290	28327	1.6
n1643-01a	w oz p	2696	2	0.1847	0.11	13.00	1.9	0.5104	1.9	1.00		2723	137	1665	104087	0.05
n1643-09b	oz og	2695	4	0.1847	0.26	12.80	1.9	0.5028	1.9	0.99		719	55	435	1073	0.077
n1643-02a	w oz p	2674	5	0.1823	0.28	12.89	1.9	0.5126	1.9	0.99		369	2	[224]	2279	0.006
n1643-10a	oz p	2670	5	0.1819	0.28	12.59	1.9	0.5020	1.9	0.99		940	150	576	1934	0.16
n1643-08a	oz p	2645	5	0.1792	0.33	11.29	1.9	0.4569	1.9	0.98	-6.3	783	106	441	1311	0.13
Data ignored due to high discordance or low $^{206}Pb/^{204}Pb$																
n1643-17a	w oz p	2819	6	0.1991	0.37	13.61	1.9	0.4956	1.9	0.98	-5.9	478	250	312	406	0.52
n1643-18a	w oz p	2721	23	0.1876	1.4	13.89	2.4	0.5371	1.9	0.79		546	10	348	871	0.018
n1643-14a	nz a	2668	19	0.1816	1.1	7.433	1.9	0.2968	1.9	0.86	-37.1	1325	105	[549]	159	0.080
n1643-11a	oz p	2581	4	0.1724	0.23	8.161	1.9	0.3433	1.9	0.99	-27.5	1029	118	430	1943	0.11
n1643-13a	mm p	2573	4	0.1716	0.26	8.013	1.9	0.3387	1.9	0.99	-28.2	1735	536	713	1279	0.31
n1643-19a	w c z p	2466	4	0.1609	0.26	7.067	1.9	0.3185	1.9	0.99	-28.9	2448	382	926	7246	0.16
n1643-09a	oz	2023	31	0.1246	1.8	8.112	2.6	0.4721	1.9	0.73	18.2	107	54	[65]	175	0.50

*oz=oscillatory zoned; nz=non zoned; mm= metamictic (often chaotically zoned); c=core; og=overgrowth; wz=weakly zoned (oscillatory zoned?); a=anhedral; i=isometric

Table 2. TIMS U-Pb zircon analyses from the Päivärinta migmatite.

Fraction	Weigth (mg)	U conc (ppm)	Pb conc (ppm)	$^{206}Pb/^{204}Pb$ measured	$^{208}Pb/^{206}Pb$ radiogenic	ISOTOPIC RATIOS*							APPARENT AGES (Ma)		
						$^{206}Pb/^{238}U$	±2σ (%)	$^{207}Pb/^{235}U$	±2σ (%)	$^{207}Pb/^{206}Pb$	±2σ (%)	ρ**	$T_{206/238}$	$T_{207/235}$	$T_{207/206}$
A79 - Päivärinta (mesosome in stromatic migmatite)															
A) ρ>4.6, long prismatic	9.2	333	149	11152	0.076	0.4074	0.65	10.951	0.65	0.1950	0.15	0.97	2203	2518	2784
B) ρ>4.6, subhedral	21.3	262	144	14368	0.072	0.5025	0.70	13.487	0.70	0.1947	0.20	0.95	2624	2714	2782
C) ρ=4.2-4.6 g cm⁻³, >150µm	12.7	563	299	6733	0.066	0.4878	0.65	12.937	0.65	0.1924	0.15	0.97	2560	2675	2762
D) ρ=4.2-4.6 g cm⁻³, long	18.3	524	278	7666	0.070	0.4860	0.70	12.864	0.70	0.1920	0.20	0.95	2553	2669	2759
E) ρ=4.0-4.2 g cm⁻³, subhedral	16.2	953	464	4166	0.061	0.4482	0.65	11.523	0.65	0.1865	0.15	0.97	2387	2566	2711
F) ρ=4.2-4.6 g cm⁻³, <150µm	13.1	536	284	4089	0.075	0.4812	0.65	12.788	0.65	0.1928	0.15	0.97	2532	2664	2765
G) ρ=4.2-4.6 g cm⁻³, <150µm/HF	13.8	437	251	31443	0.079	0.5234	0.65	14.120	0.65	0.1957	0.15	0.97	2713	2757	2790
A80 - Päivärinta (leucosome in stromatic migmatite)															
A) ρ>4.6, <150µm	10.2	242	124	819	0.064	0.4503	0.65	11.543	0.65	0.1859	0.15	0.97	2399	2569	2706
B) ρ=4.2-4.6 g cm⁻³, >150µm	12.9	665	345	1373	0.038	0.4738	0.65	12.251	0.65	0.1875	0.15	0.97	2500	2623	2720
C) ρ=4.2-4.6 g cm⁻³, <150µm	21.7	635	328	792	0.048	0.4573	0.65	11.692	0.65	0.1854	0.36	0.92	2427	2580	2702
D) ρ=4.0-4.2 g cm⁻³, >150µm	15.7	898	473	1230	0.039	0.4786	0.65	12.400	0.65	0.1879	0.15	0.97	2520	2635	2724
E) ρ=3.8-4.0 g cm⁻³, >150µm	15.1	1360	619	745	0.041	0.4052	0.65	10.078	0.65	0.1804	0.15	0.97	2192	2441	2656
F) ρ=3.6-3.8 g cm⁻³, <150µm	9.1	1625	481	322	0.057	0.2425	0.77	5.501	0.99	0.1649	0.53	0.80	1399	1902	2506

*) Isotopic ratios corrected for fractionation, blank (ca. 1 ng) and age related common lead.
**) Error correlation for $^{207}Pb/^{235}U$ vs. $^{206}Pb/^{238}U$

medium grained and pinkish leucocratic granite having quartz and potassium feldspar as the main minerals.

4. Analytical methods

Migmatite samples weighing 5 to 15 kg were sawn, washed, crushed, sieved, and handled with a wet concentrating table or panning. The separation procedure for samples A404 and A405 is described by Luukkonen (1985). For this study, zircons were separated by using heavy liquids (methylene di-iodide and Clerici® solutions). For SIMS analyses, zircons were hand-picked and mounted in epoxy resin together with chips of zircon standard (91500; Wiedenbeck et al., 1995). The mounted grains were then sectioned in half and polished. Backscattered electron images (BSE) and cathodoluminesence (CL) imaging were performed in order to assess the internal structures of crystals (Fig. 4). For selected grains, high spatial resolution U-Th-Pb data were gathered using a Cameca IMS1270 ion microprobe at the Swedish Museum of Natural History, Stockholm (NORDSIM facility). The analytical procedure follows that described by Whitehouse et al. (1999) and Whitehouse and Kamber (2005). The U/Pb data were calibrated against a 91500 zircon standard (Wiedenbeck et al., 1995) and corrected for background at mass 204.2 and modern common lead (T=0; Stacey & Kramers, 1975).

For conventional multigrain U-Pb analyses the decomposition of zircons and extraction of U and Pb mainly followed the procedure described by Krogh (1973). U and Pb isotopic ratios were measured using a thermal ionisation multicollector mass spectrometer (TIMS) in the Geological Survey of Finland, Espoo. These analyses were made during 1981 and 1982. Analytical procedures used for the conventional multigrain U-Pb analyses are described in detail by Vaasjoki (2001).

The SIMS results are reported in Table 1 at 1σ error level; all the errors quoted in the text are at 2σ error level. The age calculations are performed and concordia plots prepared using Isoplot v. 3.00 software of Ludwig (2003).

5. U-Pb age results and interpretation of the ages

5.1. Mesosome A1815

The zircons in sample A1815 are mostly transparent, oscillatory zoned, long prisms with rare overgrowths (Fig. 4). A minority of the grains are metamict. A total of 29 spots, representing 29 grains, were analysed from the sample. Five analyses were ignored due to high discordance and/or low $^{206}Pb/^{204}Pb$ (Table 1). Nineteen of the analyses are concordant, of which 17 analyses define a concordia age of 2803 ± 4 Ma (Fig. 5a). The five slightly discordant analyses have $^{207}Pb/^{206}Pb$ ages between 2810 ± 14 Ma and 2777 ± 10 Ma. The two remaining analyses are from partially metamict (destroyed primary oscillatory zoning?) and oscillatory zoned zircons, respectively. These two analyses define a concordia age of 2739 ± 8 Ma.

Interpretation: The age of 2803 ± 4 Ma is considered to represent the igneous age of the protolith and the two-point age of 2739 ± 8 Ma is assigned to some later event of radiogenic lead-loss or metamorphism.

5.2. Leucosome A1816

The zircons in sample A1816 are mainly short, subhedral and reddish prisms. BSE and CL images revealed strong metamict character (Fig. 4) and destruction of primary zoning in most of the zircons. A total of 18 spots, representing 17 grains, were dated. Of the resultant data points only three are concordant at the 2σ error level (Fig. 5b). One of these three was ignored due to low $^{206}Pb/^{204}Pb$. The remaining two concordant analyses have $^{207}Pb/^{206}Pb$ ages of 2699 ± 6 Ma and 2682 ± 4 Ma.

Interpretation: Based on these data, no reliable age estimate can be made. However, we consider that the concordant ages of ca. 2.70 Ga and 2.68 Ga are probably related to the leucosome formation event.

5.3. Mesosome A1765

Most of the zircons are euhedral and transparent long prisms. BSE and CL images reveal oscillatory zoning
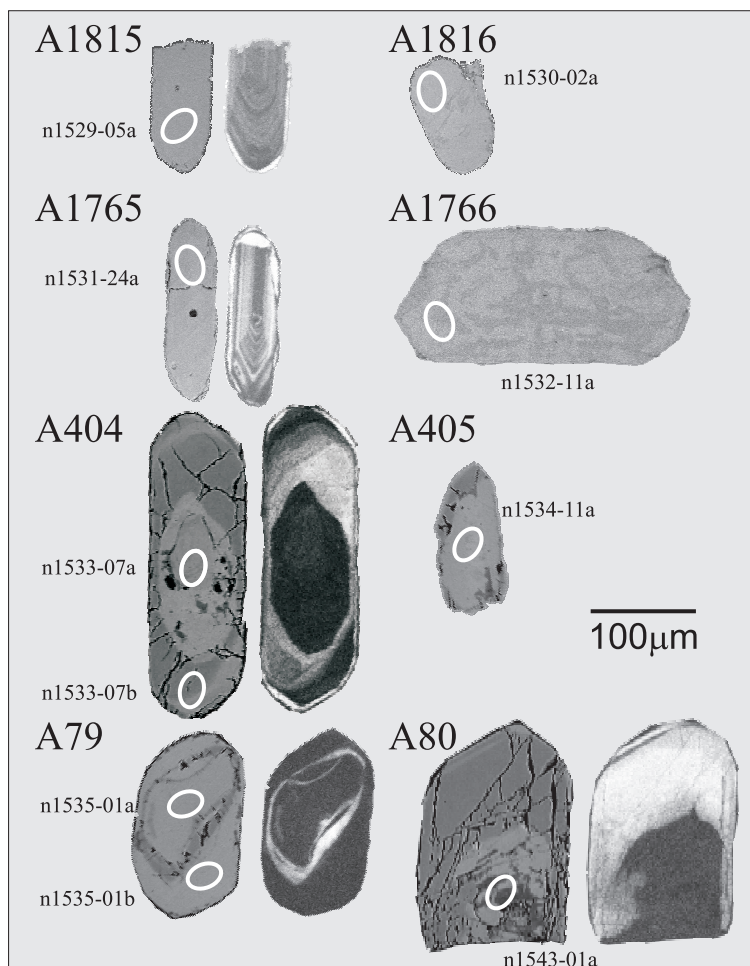
Fig. 4. Back-scattered electron and cathodoluminescence images on representative zircons with spot locations marked.

in most of the grains (Fig. 4). Some of the grains have very thin homogeneous overgrowths. A total of 20 points, representing 20 grains, were analysed. Twelve of these data are concordant at 2σ error level (Fig. 5c). Ten of the concordant analyses form a distinct cluster that yields a concordia age of 2792 ± 6 Ma. The two distinct concordant analyses, n1531-10a and n1531-06a, show older $^{207}Pb/^{206}Pb$ ages of 2828 ± 10 Ma and 2845 ± 10 Ma, respectively.

Interpretation: Due to the homogeneity of the population, the age of 2792 ± 6 Ma is considered to be the age of the igneous protolith, and the older zircons are attributed to inheritance.

5.4. Leucosome A1766

The zircons in leucosome A1766 are mostly transparent, long prisms. In BSE and CL images some of the zircons show oscillatory zoning, whereas most of the zircons are metamict with destroyed zoning structures (Fig. 4). A total of 25 points, representing 25 grains, were analysed. Six of the analyses were discarded due to high discordance and/or low $^{206}Pb/^{204}Pb$. Eight of the remaining 19 analyses are concordant within 2σ error levels (Fig. 5d). Concordant and nearly concordant data form two separate clusters and reveal a heterogeneous zircon population within the sample. The older cluster consists of grains that have $^{207}Pb/$ ^{206}Pb ages between ca. 2.78 Ga and 2.84 Ga, thus

being similar to the grains in the main age population of the corresponding mesosome (A1765). The youngest concordant and nearly concordant analyses yield $^{207}Pb/^{206}Pb$ ages between of ca. 2.68 Ga and 2.71 Ga (Fig. 5d)

Interpretation: Grains with ages of ca. 2.78 Ga and 2.84 Ga are considered to have been inherited, and grains with ages of ca. 2.68 Ga and 2.71 Ga are likely to be related to the prolonged leucosome generation event.

5.5. Mesosome A404

Morphological descriptions and conventional TIMS data for zircons from sample A404 were previously reported by Luukkonen (1985). BSE and CL images for this study reveal that zircons in the sample A404 commonly have cores that often are oscillatory zoned and rimmed by weakly zoned or homogeneous overgrowths (Fig. 4). A total of 14 points, representing 10 grains, were analysed. Two of the core data points show slight reverse discordance (Fig. 6a). Six of the cores have a calculated concordia age of 2942 ± 6 Ma. Two of the cores yielded significantly younger $^{207}Pb/^{206}Pb$ ages of 2833 ± 9 Ma and 2867 ± 15 Ma. A weakly oscillatory zoned zircon (possibly core) yields an age of 2898 ± 10 Ma. All of the four analysed overgrowths have low Th/U. Three of the youngest overgrowths plot in a cluster with a calculated concordia age of 2812 ± 8 Ma, and an older concordant analysis has a $^{207}Pb/^{206}Pb$ age of 2839 ± 7 Ma.

Interpretation: The age of 2942±6 Ma is considered as the maximum age of the igneous protolith and the overgrowths with low Th/U are considered to register a metamorphic event between 2.84 and 2.81 Ga.

5.6. Leucosome A405

CL images of the zircons in the sample A405 reveal relict primary oscillatory zoning within grains that are mostly metamict (Fig. 4). In CL images zircons are nearly black due to exceptionally high U contents (1333 and 6460 ppm; Fig. 7b). Thirteen analyses representing 13 grains were analysed. Analyses mostly show reverse discordance (Fig. 6b). The $^{207}Pb/^{206}Pb$ ages of the zircons vary between 2739 Ma and 2232 Ma and show a negative correlation with U and U+Th concentrations (Fig. 8 a and b).

Interpretation: Based on these data no reasonable age estimate for leucosome generation can be presented. A titanite fraction from a granodiorite dike that crosscuts both leucosome (A405) and mesosome (A404) has a slightly discordant $^{207}Pb/^{206}Pb$ age of 2662 ± 20 Ma (Luukkonen, 1985); which can be considered to constrain the minimum age of the leucosome formation event. Therefore, the younger $^{207}Pb/^{206}Pb$ ages (< 2.64 Ga) obtained from zircons cannot be reasonably attributed to any significant tectonothermal episode. The negative correlation of $^{207}Pb/^{206}Pb$ ages with U and U+Th concentrations is most probably because of radiogenic Pb-loss at some unspecified but likely relatively ancient time. It is proposed that such Pb-loss of high U zircons does not necessarily require any distinct tectonothermal event, and it could possibly be related to uplift and erosion of the migmatites. The reverse discordance is probably an analytical artefact related to high U zircons affecting the Pb/U calibration (cf. McLaren et al., 1994).

5.7. Mesosome A79

The zircons in sample A79 are generally prismatic, subhedral and transparent. BSE and CL images reveal oscillatory zoning in most of the zircons. Some grains have roundish oscillatory zoned cores with weakly zoned or homogeneous overgrowths (Fig. 4). The multigrain zircon fractions analysed by TIMS are discordant and the analyses exhibit relatively wide scatter in the concordia plot (Fig. 6c). A total of 26 spots representing 22 grains were analysed by SIMS. One determination, n1644-21b, was ignored due to low $^{206}Pb/^{204}Pb$. Most of the remaining analyses are concordant and the majority of them plot between 2.83 Ga and 2.84 Ga on a concordia diagram (Fig. 6c). Four of the concordant analyses have $^{207}Pb/^{206}Pb$ ages between ca. 2.79 and 2.81 Ga. The youngest zir-
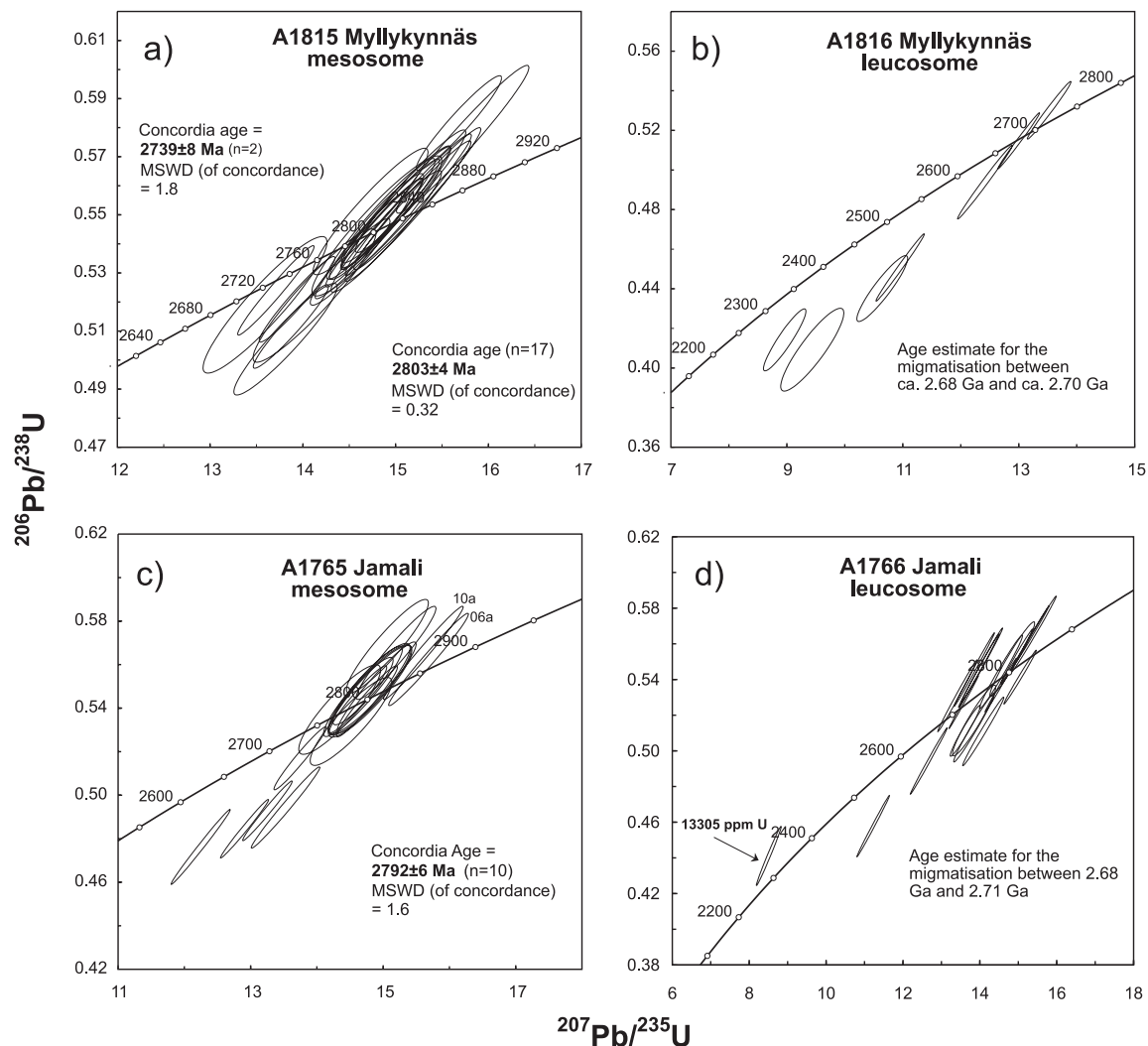
Fig. 5. Concordia diagram showing U-Pb isotopic data for samples a) A1815, b) A1816, c) 1765, and d) A1766. Data being more than 10 % discordant and/or having ^{206}Pb/^{204}Pb below 900 are not plotted (see Table 1). Ellipses indicate 2 σ errors.

con domains are the overgrowths (n=4) having ^{207}Pb/^{206}Pb ages between 2726 ± 8 Ma and 2698 ± 4 Ma. The Th/U ratios of these zircons vary between 0.25 and < 0.001 which are mostly lower than in the other zircons in the sample.

Interpretation: The igneous protolith is considered to have an age between 2.84 and 2.83 Ga, perhaps even as young as ca. 2.79 Ga. The ca. 2.73 – 2.70 Ga overgrowths are most likely related to metamorphism.

5.8. Leucosome A80

The zircons in sample A80 are prismatic, anhedral or subhedral. Most of the grains are transparent and some grains were coloured with reddish pigment. On BSE and CL images most of the grains reveal weak or no oscillatory zoning. Most of the zircons were partially or totally metamict and some zircons show rim and core structures (Fig. 4). The multigrain fractions analysed by TIMS are all discordant, and a reference
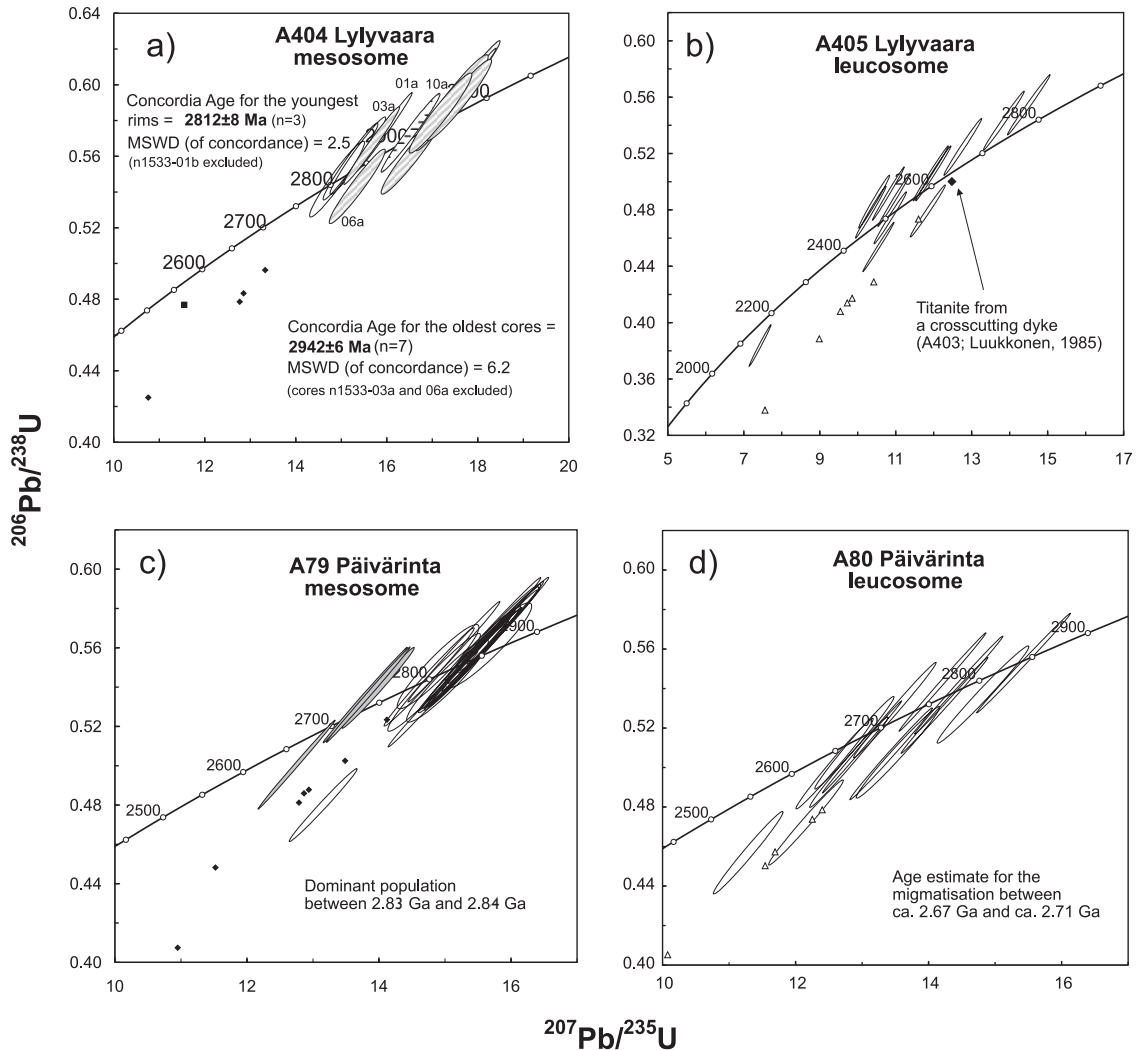
Fig. 6. Concordia diagram showing the U-Pb isotopic data for the samples a) A404 (cores = grey rastering; overgrowths/rims = open ellipses), b) A405, c) A79 (overgrowth = grey), and d) A80. Data being more than 10 % discordant and/or having $^{206}Pb/^{204}Pb$ below 900 are not plotted (see Table 1). The conventional U-Pb data for A404 and A405 (black diamonds and white triangles) and titanite (black square) are from Luukkonen (1985) and data for A79 and A80 are from Table 2. Ellipses are at 2σ level.

line with an age of 2.76 Ga may be fitted through the four most concordant fractions (reference line not shown in Fig. 6d). A total of 21 spots, representing 20 zircon grains, were analysed by SIMS. Seven analyses were ignored due to low $^{206}Pb/^{204}Pb$ and/or high discordance. Ten of the analyses are concordant within 2σ error levels (Fig. 6d). The youngest concordant zircons have $^{206}Pb/^{204}Pb$ ages between 2670 ± 10 Ma

and 2698 ± 6 Ma. The rest of the concordant analyses show $^{207}Pb/^{206}Pb$ ages between 2740 ± 4 Ma and 2846 ± 4 Ma.

Interpretation: The grains having ages of ca. 2.74 – 2.85 Ga are considered to have been inherited and the grains with ages ca. 2.67 – 2.70 Ga are probably related to the leucosome formation event.

6. Discussion

6.1. Age of migmatisation and its relation to magmatism and high-grade metamorphism in adjacent areas

The zircons analysed in leucosomes frequently have lower Th/U and higher U abundances than those in mesosomes (Fig. 7 a–d; Table 1). The majority of the zircons from leucosomes have U contents in excess of 1000 ppm, with a maximum of up to 13305 ppm (n1532-03a; Table 1). The 2.84 – 2.81 Ga overgrowths on the ca. 2.94 Ga zircon cores in the mesosome sample A404 have exceptionally low Th/U (Fig. 7b). Due to their homogeneous or weakly zoned ap-

pearance in CL images, these overgrowths are considered to register a metamorphic event. In the other three mesosome samples neither zircon cores of 2.94 Ga nor overgrowths of 2.84 – 2.81 Ga in age were observed. The 2.84 – 2.81 Ga metamorphic event registered by A404 is of similar age as the emplacement ages for some of the tonalite plutons in the Archaean of eastern Finland (cf. Lauri et al., 2006; Vaasjoki et al., 1999; Käpyaho et al., 2006), which may imply that these magmatic and metamorphic events were related to the same tectonothermal event.

Homogeneous overgrowths on 2.84 – 2.83 Ga cores in mesosome A79 were found to have $^{207}Pb/^{206}Pb$ ages between 2726 ± 8 Ma and 2698 ± 4 Ma.
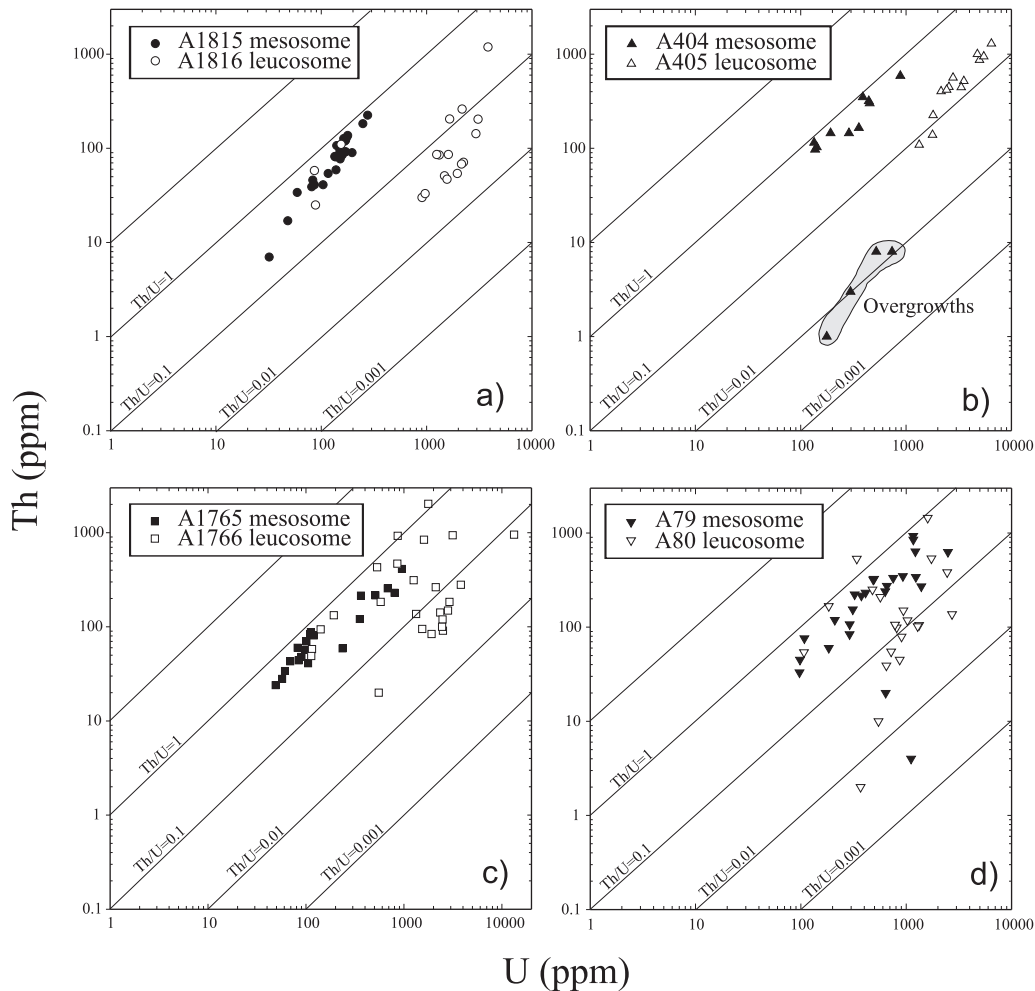
Fig. 7. U versus Th diagram showing compositional variation for the zircons of mesosome and leucosome samples dated by SIMS.

The Th/U of these overgrowths is generally low, varying from 0.01 to 0.25 (Fig. 7d). It is worth noting that the ages of these overgrowths are similar to those of titanites and monazites reported from Archaean rocks of eastern Finland and Russian Karelia, which are usually considered to date metamorphism or cooling of the crust following magmatic events (Vaasjoki et al., 1993; Bibikova et al., 2001; Käpyaho et al., 2006; Lauri et al., 2006).

Because of the scarcity of concordant U-Pb data for the leucosomes, only tentative estimates of the migmatisation ages could be made based on the individual dated samples. Furthermore, the youngest ages of individual leucosome samples A1816, A1766 and A80 scatter within 20 – 30 Ma. The available data do not allow us to conclude whether all of the leucosomes studied were formed synchronously in a single prolonged tectonothermal event, or whether they represent products of separate magmatic events. All these ages, however, are within the age interval of 2.71 – 2.67 Ga. Given that anatectic conditions in the crust may persist over an extended period of time (> 30 Ma; Rubatto et al., 2001), it is most likely that the U-Pb results from the three leucosome samples are indicative of continuous partial melting during a high-grade metamorphic event, that started ca. 2.72 Ga and continued until at least to 2.67 Ga.

The majority of the youngest Neoarchaean plutonic rocks (mostly leucogranites and granodiorites) in eastern Finland and adjacent Russian Karelia have ages between ca. 2.70 and 2.68 Ga (Bibikova et al., 2003; Käpyaho et al., 2006; Lauri et al., 2006). These ages are similar to the assumed leucosome formation event. On several occasions it has been interpreted that the ca. 2.70 – 2.68 Ga leucocratic granitoid rocks in eastern Finland contain a notable recycled component, with variable, often probably minor, additions of juvenile material (e.g. Luukkonen, 1988; Käpyaho et al., 2006; Lauri et al., 2006). Based on the presence of inherited zircons in the leucosomes, it is also likely that the leucosome material is at least partly derived from melting of pre-existing crustal material. This seems particularly likely for the Jamali migmatite, where the leucosome material contains an inherited zircon population with an age distribution very similar to that of the oldest zircon population in the mesosome. Although it is impossible to set undisputable age constraints for the leucosome forming event, we consider it likely that the migmatisation and the ca. 2.70 – 2.68 Ga plutonism throughout eastern Finland were related to the same tectonothermal event.
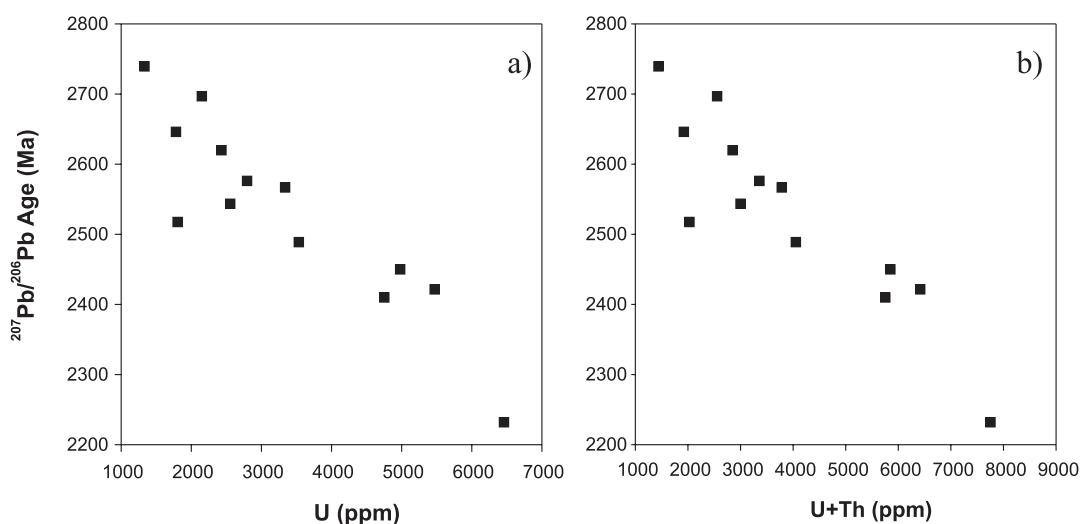
Fig. 8. a) U versus ^{207}Pb/^{206}Pb age and b) Th+U versus ^{207}Pb/^{206}Pb age diagrams for zircons from sample A405.

Low Th/U zircon overgrowths with U-Pb ages of 2.67 – 2.63 Ga have commonly been reported for granites, granodiorites and paragneisses from eastern Finland (Käpyaho et al., 2006; Kontinen et al., 2007). These overgrowths have broadly similar ages to the monazites and zircons from the Varpaisjärvi area (Iisalmi block in Fig. 1), which were considered to register a metamorphic event (Hölttä et al., 2000; Mänttäri & Hölttä, 2002). **Kontinen et al. (2007)** proposed that the zircon overgrowths having ages of 2.66 – 2.63 Ga are probably related to late stages of accretion or cratonisation of the crust. These ages are, however, younger than the 2.72 – 2.70 Ga low Th/U overgrowths observed in the Päivärinta mesosome (sample A79). If the leucosomes have crystallized at ca. 2.72 – 2.67 Ga, as it seems, then zircon over-

growths must have formed both before and after the main magmatic event. The available age data is still too scarce to ascertain whether the period from 2.72 – 2.63 Ga involved one or more tectonothermal pulses, although the latter alternative is considered likely.

6.2. Migmatite protolith ages, and their implications for the tectonic evolution of the western part of the Karelian craton

According to the summary by Van Kranendonk (2004), it is impossible to generalise as to whether or not Archaean greenstone belts are autochthonous or allochthonous in their present tectonic positions. This classical problem is also relevant in the case of the Kuhmo greenstone belt, for which various tecton-
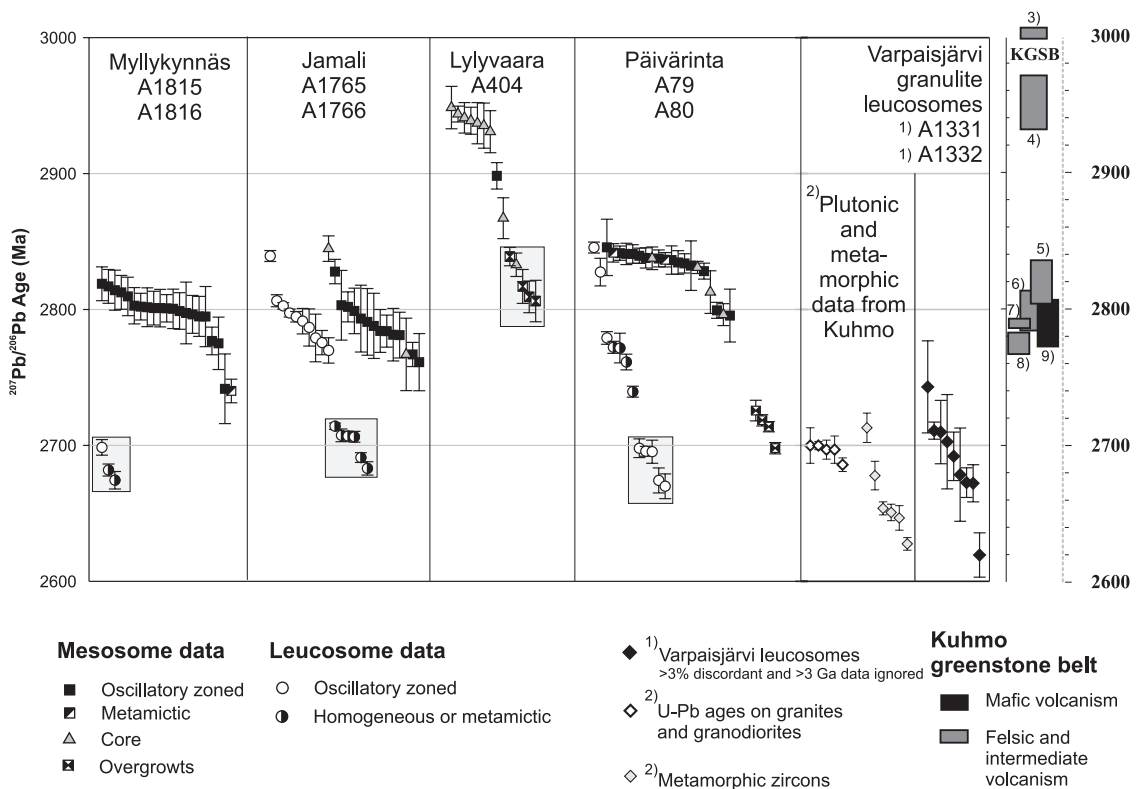
Fig. 9. Cumulative plot of $^{207}Pb/^{206}Pb$ ages with 2σ error bars showing data on leucosomes and mesosomes from Archaean migmatites in eastern Finland. Analyses are arranged in order of consecutive age. Data > 3 % discordant are ignored (Table 1). Data sources: 1) Mänttäri & Hölttä (2002), data > 3 % discordant and older than 3 Ga ignored; 2) Käpyaho et al. (2006), note that U-Pb ages with 2σ error bars are shown the for granites and granodiorites; 3) A120, Luukkonen et al. (2002); 4) A1467, Luukkonen et al. (2002); 5) A1428, Luukkonen et al. (2002); 6) A511, Hyppönen (1983); 7) A1174, Vaasjoki et al. (1999); 8) A1429, Luukkonen et al. (2002); 9) A976, Luukkonen (1988).

ic scenarios have been proposed (see Chapter 1). The U-Pb data presented in this study may give some constraints for the modelling of the origin of the Kuhmo greenstone belt. In the case of an intracontinental rift model, an older basement for the volcanism of the greenstone belt would be expected. Luukkonen (1992) suggested that such basement would be represented by the banded amphibolites within the migmatite complexes. Their age was considered older than the conventional U-Pb age of 2843 ± 18 Ma obtained for the Lylyvaara migmatite mesosome (sample A404), as this age was considered to represent the age of metamorphism (Luukkonen, 1985). The SIMS data presented in this study confirm that the zircons in A404 do indeed have older cores (Figs. 4, 6a and 9), with a calculated concordia age of 2942±6 Ma for the oldest grains. This age is broadly coeval or slightly younger with the oldest reported volcanic rocks (ca. 2.95 – 3.0 Ga; Luukkonen et al., 2002) within the northernmost part of the belt (i.e. Suomussalmi in Figs. 1 and 10). Therefore, the Lylyvaara-type migmatite mesosomes may have provided a depositional basement for the ca. 2.8 Ga volcanic rocks, but not for the apparently oldest (> 2.95 Ga) volcanic rocks of the Kuhmo-Suomussalmi greenstone belt.

The protolith ages of the three other mesosomes (A1815, A1765, and A79) are younger than the A404. In sample A79, most of the zircons have ages of ca. 2.83 – 2.84 Ga, whereas most of the zircons in samples A1815 and A1765 are as much as 30 – 40 Ma younger (Fig. 9). Consequently, the mesosomes seem to have different U-Pb ages, confirming that the migmatites of the gneiss complexes in eastern Finland are heterogeneous in terms of their protolith ages. The migmatite protoliths appear to derive from rocks that were formed contemporaneously with most of the dated mafic and felsic volcanic rocks within the Kuhmo greenstone belt (Fig. 9). This could mean that some of the migmatite complexes surrounding the greenstone belt may in fact consist of igneous and/or sedimentary material correlative with those in the greenstone belt.

Genetic models for the evolution of the Archaean crust in the eastern Finland have recently fa-
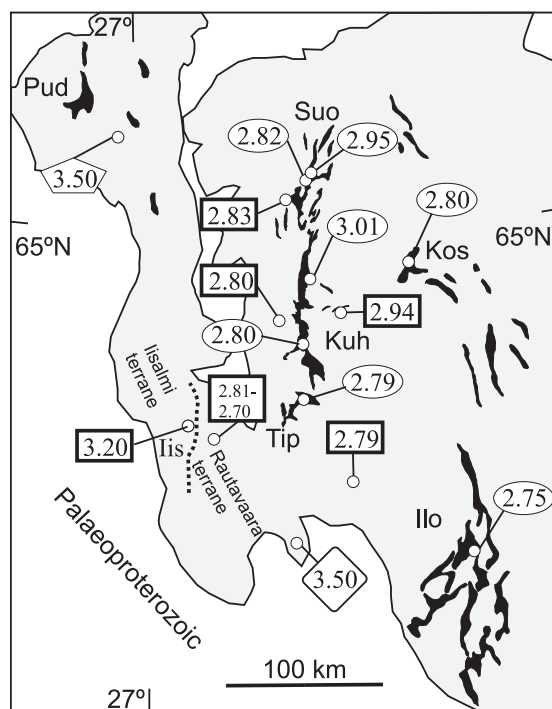
Fig. 10. Generalised bedrock map (modified after Korsman et al., 1997) showing U-Pb ages on migmatite mesosomes (squares), metavolcanic rocks (ellipses), gneiss from Pudasjärvi (pentagon) and lower crust (diamond). Abbreviations are as in Fig. 1. Data sources for the mesosomes are from Mänttäri & Hölttä (2002); this study, and for metavolcanic rocks from Hyppönen (1983); Vaasjoki et al. (1999); Luukkonen et al. (2002), and for Pudasjärvi Mutanen & Huhma (2003), and lower crustal xenolith data after Peltonen et al. (2006).

voured the concept of Archaean orogenesis culminating in continent-continent collisional and accretionary process (Kontinen & Paavola, 2006). Kontinen & Paavola (op.cit.) proposed that this collisional event took place at ca. 2.7 Ga, when the Pudasjärvi-Iisalmi and Kuhmo-Ilomantsi blocks were amalgamated (Figs. 1 and 10). Earlier, Hölttä (1997) and Mänttäri & Hölttä (2002) proposed that the Rautavaara terrane with < 2.80 Ga protolith ages from migmatites and gneisses was accreted to the 3.2 Ga Iisalmi terrane (Fig. 10). The possible continuation of the Iisalmi terrane to north and south are not presently known, but the presence of the ca. 3.5 Ga Siurua gneisses demonstrates that Mesoarchaean to Palaeoarchaean crust is at least locally present north of

the Iisalmi terrane, in the Pudasjärvi block (Mutanen & Huhma, 2003). Cordierite-orthoamphibole rocks containing zircons that have U-Pb ages < 2.80 Ga are present in the Rautavaara terrane (Figs. 1 and 10), but seems to lack from the Kuhmo region. Taking the available data together, mesosomes of migmatites from Kuhmo region (including the Nurmes belt; cf. Kontinen et al., 2007) seem to be younger than those observed from Iisalmi terrane (cf. Mänttäri & Hölttä). On the basis of these lithological and age differences, it could be that the Kuhmo district and the Iisalmi terrane indeed have had independent tectonic histories prior to a major shared metamorphic and migmatisation event. The data presented in this paper are thus consistent with the previous hypothesis that the Archaean crust in Karelia was formed by accretion of crustal blocks (e.g., Hölttä, 1997; Mänttäri & Hölttä, 2002; Kontinen & Paavola, 2006). However, confirmation of this paradigm needs more age determinations.

8. Conclusions

The U-Pb data on four migmatite leucosome-mesosome pairs from eastern Finland enable us to make the following conclusions:

1) Migmatite mesosomes yielded 2.94 Ga and 2.84 – 2.79 Ga protolith ages. The 2.94 Ga protolith ages were recorded from only one sample taken from the eastern side of the Kuhmo greenstone belt. U-Pb analyses on zircons from two separate mesosome samples revealed two metamorphic periods with ages of 2.84 – 2.81 Ga and 2.73 – 2.70 Ga. These zircon overgrowths have mostly low Th/U. The latter event is interpreted to correspond to the initial stages of the high-grade metamorphic event. Based on the U-Pb analyses on zircons from leucosomes, no single event for the migmatisation could be defined. The youngest zircons from three leucosome samples have ages between 2.72 Ga and 2.67 Ga, and this age range is attributed to continuous partial melting i.e. leucosome formation, over tens of millions of years.

2) U-Pb data indicate that the mesosomes have different formation ages, which broadly correspond

to U-Pb ages obtained for volcanic rocks from the adjacent Kuhmo greenstone belt. This is considered to indicate that some of the migmatite mesosomes could represent igneous materials correlative with those from the Kuhmo greenstone belt.

References

Alapieti, T., 1982. The Koillismaa layered igneous complex, Finland – its structure, mineralogy and geochemistry, with emphasis on the distribution of chromium. Geological Survey of Finland, Bulletin 319, 116 p.

Bibikova, E., Skiöld, T., Bogdanova, S., Gorbatschev, R. & Slabunov, A., 2001. Titanite-rutile thermochronometry across the boundary between the Archaean Craton in Karelia and the Belomorian Mobile Belt, eastern Baltic Shield. Precambrian Research 105, 315–330.

Bibikova, E.V., Samsonov, A.V., Shchipansky, A.A., Bogina, M.M., Gracheva, T.V. & Makarov, V.A., 2003. The Hisovaara structure in the northern Karelian greenstone belt as a late Archean island arc: Isotopic geochronological and petrological evidence. Petrology 11, 261–290.

Bibikova, E.V., Petrova, A. & Claesson, S., 2005. The temporal evolution of sanukitoids in the Karelian Craton, Baltic Shield: an ion microprobe U-Th-Pb isotopic study of zircons. Lithos 79, 129–145.

Evins, P.M., Mansfeld, J. & Laajoki, K., 2002. Geology and geochronology of the Suomujärvi complex: a new Arche-

an gneiss region in the NE Baltic Shield, Finland. Precambrian Research 116, 285–306.

Gaál, G. & Gorbatschev, R., 1987. An outline of the Precambrian evolution of the Baltic Shield. Precambrian Research 35, 15–52.

Halla, J., 2002. Origin and Paleoproterozoic reactivation of Neoarchean high-K granitoid rocks in eastern Finland. Annales Academiae Scientiarum Fennicae, Geologica-Geographica 163, 103 p.

Halla, J., 2005. Late Archean high-Mg granitoids (sanukitoids) in the southern Karelian domain, eastern Finland: Pb and Nd isotopic constraints on crust–mantle interactions. Lithos 79, 161–178.

Halliday, A.N., Luukkonen, E.J. & Bowes., D.R., 1988. Rb-Sr whole-rock isotopic study of late Archaean and early Proterozoic granitoid intrusions, Kainuu, eastern Finland. Bulletin of the Geological Society of Finland 60, 107–113.

Hölttä, P., 1997. Geochemical characteristics of granulite facies rocks in the Archean Varpaisjärvi area, central Fennoscandian Shield. Lithos 40, 31–53.

Hölttä, P. & Paavola, J., 2000. P-T-t developement of Archean granulites in Varpaisjärvi, Central Finland, I. Effects of multiple metamorphism on the reaction history of mafic rocks. Lithos 50, 97–120.

Hölttä, P., Huhma, H., Mänttäri, I. & Paavola, J., 2000. P-T-t developement of Archaean granulites in Varpaisjärvi, Central Finland II. Dating of high-grade metamorphism with the U-Pb and Sm-Nd methods. Lithos 50, 121–136.

Huhma, H., Mänttäri, I. & Vaasjoki, M., 1999. Dating the Finnish Archaean greenstone belts – isotope geology. In: Papunen, H. & Eilu, P. (eds.) Joint field excursions and workshop of the GEODE subprojects: Archaean greenstone belts and ore deposits, Palaeoproterozoic greenstone belts and ore deposits. Institute of Geology and Mineralogy Publication No. 42, University of Turku, pp. 72–74.

Hyppönen, V., 1983. Ontojoki, Hiisijärvi and Kuhmo. Explanation to the Geological map of Finland 1:100 000, pre-Quaternary rocks, sheets 4411, 4412, 4413, Geological Survey of Finland, 60 p. (in Finnish with English summary).

Käpyaho, A., 2006. Whole-rock geochemistry of some tonalite and high Mg/Fe gabbro, diorite, and granodiorite plutons (sanukitoid suites) in the Kuhmo district, eastern Finland. Bulletin of the Geological Society of Finland 78, 121–141.

Käpyaho, A., Mänttäri, I. & Huhma, H., 2006. Growth of Archaean crust in the Kuhmo district, eastern Finland: U–Pb and Sm–Nd isotope constraints on plutonic rocks. Precambrian Research 146, 95–119.

Koistinen, T., Stephens, M.B., Bogatchev, V., Nordgulen, Ø., Wennerström, M. & Korhonen, J., (eds.), 2001. Geological map of the Fennoscandian Shield, scale 1:2 000 000. Geological Surveys of Finland, Norway,

Sweden and the North-West department of Natural Resources of Russia.

Kontinen, A. & Paavola, J., 2006. A preliminary model of the crustal structure of the eastern Finland Archaean complex between Vartius and Vieremä, based on constraints from surface geology and FIRE 1 seismic survey. In: Kukkonen, I. & Lahtinen, R. (eds.) Finnish reflection experiment. FIRE 2001–2005. Geological Survey of Finland, Special Paper 43, 223–240.

Kontinen, A., Paavola, J. & Lukkarinen, H., 1992. K-Ar ages of hornblende and biotite from late Archaean rocks of eastern Finland – interpretation and discussion of tectonic implications. Geological Survey of Finland, Bulletin 365, 31 p.

Kontinen, A., Käpyaho, A., Huhma, H., Karhu, J., Matukov, D.I., Larionov, A. & Sergeev, S., 2007. Nurmes paragneisses in eastern Finland, Karelian craton: Provenance, tectonic setting and implications for Neoarchaean craton correlation. Precambrian Research 152, 119–148.

Korsman, K., Koistinen, T., Kohonen, J., Wennerström, M., Ekdahl, E., Honkamo, M., Idman, H. & Pekkala, Y., (eds.), 1997. Suomen kallioperäkartta/Bedrock map of Finland 1:1 000 000. Geological Survey of Finland, Espoo.

Krogh, T.E., 1973. A low-contamination method for hydrothermal decomposition of U and Pb for isotopic age determinations. Geochimica et Cosmochimica Acta 37, 485–494.

Lauri, L.S., Rämö, O.T., Huhma, H., Mänttäri, I. & Räsänen, J., 2006. Petrogenesis of silicic magmatism related to the ~ 2.44 Ga rifting of Archean crust in Koillismaa, eastern Finland. Lithos 86, 137–166.

Lobach-Zhuchenko, S. B., Chekulayev, V. P., Sergeev, S. A. Levchenkov. O. A. & Krylov., I. N., 1993. Archaean rocks from southeastern Karelia (Karelian granite greenstone terrain). Precambrian Research 62, 375–397

Ludwig, K.R., 2003. Isoplot/Ex rev. 3.00. Special publication No.4. Berkeley Geochronology Center, 70 p.

Luukkonen, E.J., 1985. Structural and U-Pb isotopic study of late Archaean migmatitic gneisses of the Presvecokarelides, Lylyvaara, Eastern Finland. Transactions of the Royal Society of Edinburgh, Earth Sciences 76, 401–410.

Luukkonen, E.J., 1988. Moisiovaara and Ala-Vuokki. Explanation to the Geological map of Finland 1:100 000, pre-Quaternary rocks, Sheets 4421, 4423+4441, 68 p. (in Finnish, with English summary)

Luukkonen, E.J., 1992. Late Archaean and early Proterozoic structural evolution in the Kuhmo-Suomussalmi terrain, eastern Finland. Annales Universitatis Turkuensis. Sarja-Ser.A.II. Biologica-Geographica-Geologica, No. 78, 37 p.

Luukkonen, E.J., 2001. Lentiira. Explanation to the Geological map of Finland 1:100 000, pre-Quaternary rocks, Sheets 4414+4432. Geological Survey of Finland, 51 p.

(in Finnish with English summary)

Luukkonen, E., Halkoaho, T., Hartikainen, A., Heino, T., Niskanen, M., Pietikäinen, K. & Tenhola, M., 2002. Itä-suomen arkeeiset alueet -hankkeen (12201 ja 210 5000) toiminta vuosina 1992–2001 Suomussalmen, Hyrynsalmen, Kuhmon, Nurmeksen, Rautavaaran, Valtimon, Lieksan, Ilomantsin, Kiihtelysvaaran, Enon, Kontiolahden, Tohmajärven ja Tuupovaaran alueella. Geological Survey of Finland, Report M19/4513/2002/1, 265 p. (in Finnish)

Mänttäri, I. & Hölttä, P., 2002. U-Pb dating of zircons and monazites from Archean granulites in Varpaisjärvi, Central Finland: Evidence for multiple metamorphism and Neoarchean terrane accretion. Precambrian Research 118, 101–131.

Martin, H., 1985. Nature, origine et évolution d'un segment de croûte continentale archéenne: contraintes chimiques et isotopiques. Exemple de la Finlande orientale. Exemple de la Finlande. Memoires et Documents du Centre Armoricain d'Etude Structurale des Socles I, Rennes, 392 p.

Martin, H., 1987. Petrogenesis of Archaean trondhjemites, tonalites, and granodiorites from eastern Finland: Major and trace element geochemistry. Journal of Petrology 28, 921–953.

Martin, H., Auvray, B., Blais, S., Capdevila, R., Hameurt, J., Jahn, B.-M., Piquet, D., Querré, G. & Vidal, P., 1984. Origin and geodynamic evolution of the Archean crust of eastern Finland. Bulletin of the Geological Society of Finland 56, 135–160.

McLaren, A.C., Fitz Gerald, J.D. & Williams, I.S., 1994. The microstructure of zircon and its influence on the age determination from Pb/U isotopic ratios measured by ion microprobe. Geochimica et Cosmochimica Acta 58, 993–1005.

Mutanen, T. & Huhma, H., 2003. The 3.5 Ga Siurua trondhjemite gneiss in the Archaean Pudasjärvi Granulite Belt, northern Finland. Bulletin of the Geological Society of Finland 75, 51–68.

Peltonen, P., Mänttäri, I., Huhma, H. & Whitehouse, M., 2006. Multi-stage origin of the lower crust of the Karelian craton from 3.5 to 1.7 Ga based on isotopic ages of kimberlite-derived mafic granulite xenoliths. Precambrian Research 147, 107–123.

Piirainen, T., 1988. The geology of the Archaean greenstone-granitoid terrain in Kuhmo, eastern Finland. In: Marttila, E. (ed.) Archaean geology of the Fennoscandian Shield: proceedings of a Finnish-Soviet symposium in Finland on July 28 - August 7, 1986. Geological Survey of Finland, Special Paper 4, 39–51.

Puchtel, I.S., Shchipansky, A.A., Samsonov, A.V. & Zhuravlev, V., 1997. The Karelian granite-greenstone terrain in Russia. In: De Wit, M., Ashwal, L.D. (eds.) Greenstone belts. Oxford Monographs on Geology and Geophysics 35, pp. 699–706.

Rubatto, D., Williams, I.S. & Buick, I.S., 2001. Zircon and monazite response to prograde metamorphism in the Reynolds Range, central Australia. Contributions to Mineralogy and Petrology 140, 458–468.

Samsonov, A.V., Bogina, M.M., Bibikova E.V., Petrova, A.Y. & Shchipansky, A.A., 2005. The relationship between adakitic, calc-alkaline volcanic rocks and TTGs: implications for the tectonic setting of the Karelian greenstone belts, Baltic Shield. Lithos 79, 83–106.

Sergeev, S.A., Bibikova, Y.V., Levchenkov, O.A., Lobach-Zhuchenko, S.B., Yakovleva, S.Z., Ovchinnikova, G.V., Neymark, L.A., Komarov, A.N., & Gorokhovskiy, B.M., 1990. Izotopnaya geokhronologiya Vodlozerskogo gneysovogo kompleksa. Isotope geochronology of the Vodlozerskiy gneiss complex. Geokhimiya 1, 73–83.

Sorjonen-Ward, P. & Luukkonen, E., 2005. Archean rocks. In: Lehtinen, M., Nurmi, P. A. & Rämö, O. T. (eds.) Precambrian geology of Finland – Key to the evolution of the Fennoscandian Shield. Developments in Precambrian Geology 14. Elsevier Science B.V., Amsterdam, pp. 19–99.

Sorjonen-Ward, P., Nironen, M. & Luukkonen, E., 1997. Greenstone associations in Finland. In: De Wit, M., Ashwal, L.D. (eds.) Greenstone belts. Oxford Monographs on Geology and Geophysics 35, pp. 677–698

Stacey, J.S. & Kramers, J.D., 1975. Approximation of terrestrial lead isotope evolution by a two-stage model. Earth and Planetary Science Letters 26, 207–221.

Taipale, K., 1988. Volcanism in the Archaean Kuhmo greenstone belt, eastern Finland. In: Marttila, E. (ed.) Archaean geology of the Fennoscandian Shield: proceedings of a Finnish-Soviet symposium in Finland on July 28 - August 7, 1986. Geological Survey of Finland, Special Paper 4, 151–160.

Taipale, K., 1983. The geology and geochemistry of the Archaean Kuhmo greenstone-granite terrain in the Tipasjärvi area, eastern Finland. Acta Universitatis Ouluensis, Series A, 151, 93 p.

Vaasjoki, M., 1988. Zircon U-Pb versus Rb-Sr whole-rock age data from eastern Finland; a critical comment on the papers of Barbey & Martin and Martin, Precambrian Research, Vol. 35, 1987. Precambrian Research 39, 217–219.

Vaasjoki, M., 2001. Three decades of U-Pb mineral analyses at the Geological Survey of Finland. In: Vaasjoki, M. (ed.) Radiometric age determinations from Finnish Lapland and their bearing on the timing of Precambrian volcano-sedimentary sequences. Geological Survey of Finland, Special Paper 33, 9–13.

Vaasjoki, M., Taipale, K. & Tuokko, I., 1999. Radiometric ages and other isotopic data bearing on the evolution of Archaean crust and ores in the Kuhmo-Suomussalmi area, eastern Finland. Bulletin of the Geological Society of Finland 71, 155–176.

Vaasjoki, M., Sorjonen-Ward, P. & Lavikainen, S., 1993. U-Pb age determinations and sulphide Pb-Pb characteristics from the late Archean Hattu schist belt, Ilomantsi, east-

ern Finland. In: Nurmi, P. & Sorjonen-Ward, P. (eds.) Geological development, gold mineralization and exploration methods in the late Archean Hattu schist belt, Ilomantsi, eastern Finland. Geological Survey of Finland, Special Paper 17, 103–131.

Van Kranendonk, M.J., 2004. Preface: Archaean Tectonics 2004: A review. Precambrian Research 131, 143–151.

Vuollo, J., 1994. Palaeoproterozoic basic igneous events in Eastern Fennoscandian Shield between 2.45 and 1.97 Ga, studied by means of mafic dyke swarms and ophiolites in Finland. Acta Universitatis Ouluensis. Series A, Scientiae Rerum Naturalium, 250 p.

Vuollo, J. & Huhma, H., 2005. Paleoproterozoic mafic dikes in NE Finland. In: Lehtinen, M., Nurmi, P.A. & Rämö, O.T. (eds) Precambrian geology of Finland – Key to the evolution of the Fennoscandian Shield. Developments in Precambrian Geology 14. Elsevier Science B.V., Amsterdam, 195–236.

Whitehouse, M.J. & Kamber, B.S, 2005. Assigning dates to thin gneissic veins in high-grade metamorphic terranes: A cautionary tale from Akilia, Southwest Greenland. Journal of Petrology 46, 291–318.

Whitehouse, M.J., Kamber, B.S. & Moorbath, S., 1999. Age significance of U-Th-Pb zircon data from early Archaean rocks of West Greenland; a reassessment based on combined ion-microprobe and imaging studies. Chemical Geology 160, 201–224.

Wiedenbeck, M., Allé, P., Corfu, F., Griffin, W.L., Meier, M., Oberli, F., von Quadt, A., Roddick, J.C. & Spiegeln, W., 1995. Three natural zircon standards for U-Th-Pb, Lu-Hf, trace element and REE analysis. Geostandards Newsletter 19, 1–23.